

# A Thermodynamic Evaluation of the Cr-Mn and Fe-Cr-Mn Systems

BYEONG-JOO LEE

A thermodynamic evaluation of the Cr-Mn and Fe-Cr-Mn systems has been made by using thermodynamic models for the Gibbs energy of the individual phases. An optimized set of thermodynamic parameters was obtained taking into consideration related experimental information. The thermodynamic parameters of the Cr-Mn and Fe-Cr-Mn systems and comparisons between calculation and experimental data are presented.

## I. INTRODUCTION

CHROMIUM and manganese are industrially important alloying elements in steels. Knowledge of the thermodynamic properties of the Fe-Cr-Mn system are essential for understanding the behavior of alloy steels, including chromium and manganese. Recently, high-manganese austenitic steels have been of great interest as a replacement for the widely used Fe-Cr-Ni stainless steels in fusion reactors, because they have a reduced level of long-time radioactivation.<sup>[1]</sup> Several experimental investigations on the phase stability of the austenite (fcc) have been reported.<sup>[2-6]</sup> However, there is a big discrepancy in the austenite stabilized region among various investigators. The phase equilibria between the fcc and sigma phases still remains uncertain. Therefore, more reliable information on the stability of fcc and the fcc/fcc+sigma phase boundary in the Fe-Cr-Mn system is necessary. A thermodynamic calculation of the bcc/fcc equilibria in the Fe-Cr-Mn system has been made by Kirchner and Uhrenius.<sup>[7]</sup> In their study, the Cr-Mn binary part and the sigma phase were not assessed and therefore the applicability of their results was limited to the Fe-rich region. No other thermodynamic calculation of the phase equilibria including the sigma phase, has been reported for this system.

The Cr-Mn binary phase diagram is characterized by the presence of the sigma phase, which occurs at about 75 to 80 at. pct Mn up to melting temperature. Three modifications have been reported for the sigma phase, each with the same  $\sigma$ -type structure but in different states of order.<sup>[8,9]</sup> The high-temperature sigma phase shows quite different equilibrium behavior from the mid- and low-temperature sigma phases; that is, there is an abrupt change in the slope of the bcc/bcc+sigma phase boundaries near the high-temperature  $\rightarrow$  mid-temperature sigma-phase transformation temperature. It has been very common to describe such a phase with one thermodynamic model and one set of thermodynamic parameters for the sake of simplicity. For example, Kaufman<sup>[10]</sup> described the Cr-Mn sigma phase as a stoichiometric compound with the composition,  $\text{Cr}_{0.21}\text{Mn}_{0.79}$ , using one Gibbs energy expression. However, the bcc/bcc+sigma phase boundaries were not reproduced well. No successful

thermodynamic calculation of the Cr-Mn binary system has been reported after Kaufman, probably due to the difficulty in reproducing the phase equilibria including the sigma phase. Therefore, the Fe-Cr-Mn ternary system has not been assessed in the whole composition range either.

The purpose of the present study is to thermodynamically evaluate the Cr-Mn binary system so that the evaluation of the Fe-Cr-Mn system becomes possible by combining the thermodynamic data of the Cr-Mn system with those of the Fe-Cr and Fe-Mn systems where thermodynamic evaluations have already been reported.<sup>[11,12]</sup> In the present study, the high-temperature modification of the sigma phase and the mid- and low-temperature modifications of the sigma phase were described as two different phases, the high-temperature sigma phase ( $h\text{-}\sigma$ ) and the ordinary sigma phase ( $\sigma$ ), respectively. The same thermodynamic model was applied, but different thermodynamic parameter values were used for the two Cr-Mn sigma phases. The thermodynamic evaluation of the Fe-Cr-Mn ternary system was also carried out.

## II. THERMODYNAMIC MODELS

The Fe-Cr-Mn system exhibits six solution phases, bcc, fcc,  $\beta$ -Mn,  $\alpha$ -Mn, liquid, sigma, and one intermediate phase,  $\alpha'$ . A subregular solution model was applied to the first five solution phases, and a sublattice model recently developed<sup>[13,14]</sup> was used for the sigma phase. The subregular solution model yields the following expression for the molar Gibbs energy of each phase.

$$G_m = y_{\text{Fe}}^{\circ} G_{\text{Fe}}^{\circ} + y_{\text{Cr}}^{\circ} G_{\text{Cr}} + y_{\text{Mn}}^{\circ} G_{\text{Mn}} + RT \cdot (y_{\text{Fe}} \ln y_{\text{Fe}} + y_{\text{Cr}} \ln y_{\text{Cr}} + y_{\text{Mn}} \ln y_{\text{Mn}}) + {}^{sv}G_m + {}^{mo}G_m \quad [1]$$

where

$${}^{sv}G_m = y_{\text{Fe}} y_{\text{Cr}} L_{\text{Fe,Cr}} + y_{\text{Fe}} y_{\text{Mn}} L_{\text{Fe,Mn}} + y_{\text{Cr}} y_{\text{Mn}} L_{\text{Cr,Mn}} + y_{\text{Fe}} y_{\text{Cr}} y_{\text{Mn}} L_{\text{Fe,Cr,Mn}} \quad [2]$$

The parameter  ${}^{\circ}G_i$  is the Gibbs energy of pure element  $i$  in a hypothetical nonmagnetic state. All of the  ${}^{\circ}G$  values are given relative to the enthalpy of selected reference states for the elements at 298.15 K. This state is denoted by stable element reference (SER). The term  ${}^{mo}G_m$  represents the contribution due to magnetic ordering in

BYEONG-JOO LEE, Senior Researcher, is with the Standard Reference Data Group, Korea Research Institute of Standards and Science, Taejon 305-606, Korea.

Manuscript submitted July 28, 1992.

the form suggested by Inden<sup>[15]</sup> and Hillert and Jarl.<sup>[16]</sup> The Curie or Néel temperature and the average magnetic moment per atom are entered as functions of composition. The Gibbs energy expression for the Cr-Mn binary phases can be obtained by giving the zero value to  $y_{Fe}$  in the previous equations.

In the previous assessment of the Fe-Cr (11) system, a three-sublattice model with formula unit  $Fe_8Cr_4(Fe,Cr)_{18}$  was used for the sigma phase. In the present assessment, the same three-sublattice model with formula unit  $Mn_8Cr_4(Cr,Mn)_{18}$  was used for the Cr-Mn binary sigma phase. Now, it is natural to combine both models to give a formula unit  $(Fe,Mn)_8Cr_4(Fe,Cr,Mn)_{18}$  for the ternary sigma phase. The Gibbs energy of one mole of formula unit can be expressed as follows:

$$\begin{aligned}
 G_m^\sigma = & \ ^1y_{Fe}^3y_{Fe}^{\circ}G_{Fe:Cr:Fe}^\sigma + \ ^1y_{Fe}^3y_{Cr}^{\circ}G_{Fe:Cr:Cr}^\sigma \\
 & + \ ^1y_{Fe}^3y_{Mn}^{\circ}G_{Fe:Cr:Mn}^\sigma + \ ^1y_{Mn}^3y_{Fe}^{\circ}G_{Mn:Cr:Fe}^\sigma \\
 & + \ ^1y_{Mn}^3y_{Cr}^{\circ}G_{Mn:Cr:Cr}^\sigma + \ ^1y_{Mn}^3y_{Mn}^{\circ}G_{Mn:Cr:Mn}^\sigma \\
 & + 8RT(^1y_{Fe} \ln ^1y_{Fe} + ^1y_{Mn} \ln ^1y_{Mn}) \\
 & + 18RT(^3y_{Fe} \ln ^3y_{Fe} + ^3y_{Cr} \ln ^3y_{Cr} + ^3y_{Mn} \ln ^3y_{Mn}) \\
 & + {}^{xs}G_m^\sigma
 \end{aligned} \quad [3]$$

where

$$\begin{aligned}
 {}^{xs}G_m^\sigma = & \ ^1y_{Fe}({}^3y_{Fe}^3y_{Cr}L_{Fe:Cr:Cr,Fe}^\sigma + {}^3y_{Fe}^3y_{Mn}L_{Fe:Cr:Fe,Mn}^\sigma \\
 & + {}^3y_{Cr}^3y_{Mn}L_{Fe:Cr:Cr,Mn}^\sigma) \\
 & + \ ^1y_{Mn}({}^3y_{Fe}^3y_{Cr}L_{Mn:Cr:Cr,Fe}^\sigma + {}^3y_{Fe}^3y_{Mn}L_{Mn:Cr:Fe,Mn}^\sigma \\
 & + {}^3y_{Cr}^3y_{Mn}L_{Mn:Cr:Cr,Mn}^\sigma) \\
 & + \ ^1y_{Fe} \ ^1y_{Mn}({}^3y_{Fe}L_{Fe,Mn:Cr:Fe}^\sigma + {}^3y_{Cr}L_{Fe,Mn:Cr:Cr}^\sigma \\
 & + {}^3y_{Mn}L_{Fe,Mn:Cr:Mn}^\sigma)
 \end{aligned} \quad [4]$$

The notations  $^1y_i$  and  $^3y_i$  refer to the site fraction of component  $i$  in the first and third sublattice, respectively. The components in different sublattices are separated by a colon and in the same sublattice by a comma. The  $^{\circ}G$  parameters are the Gibbs energies of the hypothetical sigma phases with each sublattice filled by only one kind of atoms and are expressed as

$${}^{\circ}G_{ij:k}^\sigma = 8^{\circ}G_i^{fcc} + 4^{\circ}G_j^{bcc} + 18^{\circ}G_k^{bcc} + \Delta^{\circ}G_{ij:k}^\sigma \quad [5]$$

following a suggestion by Andersson *et al.*<sup>[17]</sup> The term  $\Delta^{\circ}G_{ij:k}^\sigma$  is a parameter to be evaluated in the assessment.

The intermediate phase  $\alpha'$  was treated as a stoichiometric compound with formula unit  $Cr_3Mn_5$ .

### III. EXPERIMENTAL INFORMATION

#### A. The Cr-Mn Binary System

The experimental information on the Cr-Mn binary system can be divided into three groups: phase equilibrium data, thermochemical data, and magnetic property data. A thorough review of the Cr-Mn system was made

recently by Venkatraman and Neumann<sup>[9]</sup> and is recommended for obtaining other information on this system which was not treated in the present study. The first systematic investigation on phase equilibria in the Cr-Mn system was reported by Kornilov and Tatyanchikova<sup>[18]</sup> in 1945. However, the phase diagram compiled by these authors shows no intermediate phase and no bcc modification of manganese. More accurate investigation on this system was made by Carlile *et al.*<sup>[19]</sup> in 1949, who determined liquidus/solidus lines using thermal analysis for the whole composition range. They also determined phase boundaries between solid phases for the composition range of 60 to 100 at. pct Mn using standard methods, such as microscopy, thermal analysis, and X-ray diffraction. Temperature measurements were carried out using an optical pyrometer. The materials used were prepared from chromium of about 99.8 wt pct purity and manganese of 99.98 wt pct purity. The experimentally determined melting point of chromium was 1845 °C, which is lower than the currently accepted value of 1907 °C.<sup>[20]</sup> They found a wide solid solution of manganese in chromium extending up to approximately 70 at. pct Mn at above 1000 °C and detected an intermediate phase at the composition range of 70 to 85 at. pct Mn and at the whole temperature range investigated, from 500 °C up to melting temperature. This intermediate phase was shown later<sup>[21]</sup> to possess the same crystal structure as the  $\sigma$  phase in the Fe-Cr system. The liquidus curve for the Cr-rich solid solution was also reported by Greenaway *et al.*<sup>[22]</sup> using the same method (thermal analysis) but a different temperature measuring technique (W/Mo thermocouple) and materials of different purity with lower oxygen and higher nitrogen contents than Carlile *et al.* The resultant liquidus points by Greenaway *et al.* were about 30 °C lower than those by Carlile *et al.* The occurrence of the sigma phase was confirmed by Zwicker,<sup>[23]</sup> whose data supported the phase boundaries by Carlile *et al.* in the Mn-rich part. His data also showed that the solubility of manganese in chromium diminishes rapidly with decreasing temperature below about 1000 °C and that there are two modifications of the sigma phase with transformation from the high-temperature phase to the low-temperature phase at 985 °C to 960 °C. The phase transformation in the sigma phase was confirmed by Pearson and Hume-Rothery<sup>[24]</sup> who gave a transformation temperature of 980 °C to 1005 °C depending on composition. They found using X-ray methods that both the high- and low-temperature sigma phases have a  $\sigma$  structure resembling that of the Fe-Cr  $\sigma$  phase. They investigated the bcc/bcc+sigma phase boundaries in much detail and also confirmed the sharp decrease of manganese solubility in chromium below 1000 °C. In addition, they suggested a probable existence of another intermediate phase whose crystal structure was similar to that of  $\alpha'$ -manganese. This phase was therefore designated  $\alpha'$ -Mn and was thought to have a composition in the region of  $CrMn_2$  and form from the Cr-rich bcc solid solution and the sigma phase by a peritectoid reaction at about 600 °C. The  $\alpha'$ -Mn phase will be denoted as  $\alpha'$  in the present study. A more detailed investigation was made by Wachtel and Bartelt<sup>[8]</sup> using magnetic susceptibility measurements. They reported that the peritectoid reaction temperature for the occurrence of

the  $\alpha'$  phase is 925 °C and the  $\alpha'$  phase has a homogeneity range of 60 to 65 at. pct Mn and undergoes a transformation to an ordered  $\alpha'$  below 600 °C. They also measured the bcc/bcc+sigma phase boundaries between about 1050 and 750 °C. Their results were in good agreement with Pearson and Hume-Rothery.<sup>[24]</sup> Wachtel and Bartelt also reported another transformation in the sigma phase at about 800 °C.

Due to slow kinetics at low temperature, the experimental data on the bcc/bcc+sigma or bcc/bcc+ $\alpha'$  below 900 °C are regarded as those from metastable equilibrium. However, it seems that there is rather good agreement among the preceding investigations concerning the Cr-rich part of the Cr-Mn phase diagram. In contrast to this agreement, there is a severe disagreement between experimental information on the phase equilibria in the Mn-rich part. In addition to the work by Carlile *et al.*<sup>[19]</sup> and Zwicker,<sup>[23]</sup> two more investigations were reported on the phase equilibria in the Mn-rich region of the Cr-Mn system, one by Hellawell and Hume-Rothery<sup>[25]</sup> using thermal analysis and the other by Lugscheider and Etmayer<sup>[26]</sup> using a high-temperature X-ray technique. The main discrepancy comes from the stability region of the fcc  $\gamma$ -Mn phase. In Carlile *et al.*'s phase diagram, the solubility of chromium in fcc manganese reaches over 14 at. pct, but in Lugscheider and Etmayer's, the maximum solubility of chromium is about 7 at. pct and in Hellawell and Hume-Rothery's it is below 1 at. pct. Hellawell and Hume-Rothery pointed out that Carlile *et al.* misunderstood the bcc stabilized region as the fcc stabilized region, and when this correction was made, both results could be reconciled with each other. However, the difference between the results of Lugscheider and Etmayer and those of Hellawell and Hume-Rothery was rather hard to explain. A brief comment on this will be given in Section IV.

Several experimental investigations on the thermodynamic properties of solid Cr-Mn alloys have been reported in the literature. Eremenko *et al.*<sup>[27]</sup> measured the activity of manganese in solid Cr-Mn alloys using a molten-salts electromotive force method. The activity of manganese at 1023 K by Eremenko *et al.* showed large positive deviations from Raoult's law. Jacob<sup>[28]</sup> measured the activity of manganese in the bcc Cr-Mn alloys at 1473 K using a Knudsen cell technique, showing slight negative deviation from Raoult's law. In a series of articles, Ranganathan and Hajra<sup>[29,30]</sup> reported manganese activities in solid Cr-Mn alloys at 1223, 1273, 1323, and 1373 K, measured using an isopiestic method. Their results showed large positive deviations from Raoult's law. Recently, Lukashenko and Sidorko<sup>[31]</sup> reported the activity of manganese in solid Cr-Mn alloys measured using the same method with Eremenko *et al.*<sup>[27]</sup> (actually they are the same authors). The results at 1070 K were similar to their earlier data at 1023 K, showing large positive deviations from Raoult's law again. A more detailed review and experimental investigation on the thermodynamic properties of Cr-Mn solid alloys were made recently by Zaitsev *et al.*<sup>[32]</sup> Using alloys of high-purity level (99.9 wt pct Cr, 99.9999 wt pct Mn) and employing a Knudsen-effusion technique under ultrahigh neutral vacuum, they measured manganese vapor pressure over the bcc alloys and alloys with compositions belonging

to the two-phase equilibrium fields in the temperature range of 1031 to 1434 K. The resultant manganese activities showed moderate positive deviation from Raoult's law at 1273 K. The phase boundaries, bcc/bcc+sigma and bcc/bcc+ $\alpha'$ , computed from the thermodynamic data were in reasonable agreement with the currently accepted phase diagram of the Cr-Mn system.<sup>[9]</sup>

The Néel temperatures of the Cr-rich bcc Cr-Mn alloys were investigated by de Vries<sup>[33]</sup> using electrical resistance and Hall effect measurements, by Hamaguchi and Kunitomi<sup>[34]</sup> using neutron diffraction, electrical resistivity, and magnetic susceptibility measurements, by Wachtel and Bartelt<sup>[8]</sup> using magnetic susceptibility measurements, by Pepperhoff and Ettwig<sup>[35]</sup> using specific heat measurements, and by Alberts and Lourens<sup>[36]</sup> using thermal expansion and bulk moduli measurements. The various investigations are in reasonable agreement with each other. Pepperhoff and Ettwig<sup>[35]</sup> also reported that the enthalpy of magnetic ordering is 5.9 J/mol for pure Cr and reaches a maximum value of approximately 500 J/mol at 8.1 at. pct Mn.

## B. The Fe-Cr-Mn Ternary System

A substantial amount of information on phase equilibria in the Fe-Cr-Mn ternary system has been reported. Investigations started with the work by Köster<sup>[37]</sup> in 1934, who reported several vertical sections at constant Cr contents up to 20 wt pct and Mn up to 30 wt pct. Subsequently, several investigations<sup>[5,6,38]</sup> were reported due to the growing interest in the engineering properties of the Fe-Cr-Mn alloys. However, most of the old experimental work was conducted using alloys of low-purity level. For example, the work by Burgess and Forgem<sup>[5]</sup> was based on alloys containing 0.1 wt pct C and 0.4 wt pct Si on average. Furthermore, the 650 °C isothermal section presented by them seemed not to be obtained from isothermal aging at that temperature. The alloys used by Schafmeister and Ergang<sup>[6]</sup> contained even more than 1 wt pct Si in many cases. Due to the lack of information on the Cr-Mn binary system, the interpretation of experimental data points was unreasonable in the low Fe content region of the 700 °C isothermal section presented in their article. More accurate experimental results were reported by Grigor'ev and Gruzdeva<sup>[39]</sup> in 1949. Using materials of rather high-purity level (>99.9 wt pct) and employing microscopy, thermal analysis, and dilatometric analysis, they investigated phase equilibria and phase transformations in Fe-Cr-Mn ternary alloys. They presented the results through vertical sections at 6, 16, 22, and 28 wt pct Mn and also presented isothermal sections at 900 °C and 1000 °C. Isothermal sections of the Fe-rich part of the Fe-Cr-Mn system at other temperatures were also reported by Tavazde *et al.*<sup>[40]</sup> They investigated 700 °C and 1100 °C isothermal sections using materials with total amount of carbon and nitrogen less than 0.08 wt pct. Shevdov and Pavlenko<sup>[41]</sup> investigated 850 °C, 750 °C, and 650 °C isothermal sections using materials with 0.05 wt pct carbon. An experimental work on the ferrite (bcc)/austenite (fcc) equilibria using alloys of even higher purity level was carried out rather recently by Kirchner and Uhrenius.<sup>[7]</sup> The purity of their alloys was over 99.99 wt pct level, and the annealing

times were between 168 hours at 950 °C and 5000 hours at 750 °C. The distribution of Cr and Mn between ferrite and austenite was measured using a microprobe. The results were presented on isothermal sections at 950 °C, 900 °C, 850 °C, 800 °C, and 750 °C with tie-lines. Another experimental work on the ferrite/austenite equilibria of the Fe-Cr-Mn system was reported recently by Okazaki *et al.*<sup>[42]</sup> Using an electron probe micro-analysis method, they measured the composition of each phase in alloys which were prepared from very pure materials and were solution treated for 1 hour at 1000 °C to 1200 °C. The phase boundaries at 1000 °C, 1100 °C, and 1200 °C were presented as lines but without data points.

As mentioned in Section I, high-manganese austenitic steels have great interest for fusion reactor structural material. Therefore, more reliable information on the stability of austenite and phase equilibria with the sigma phase in the Fe-Cr-Mn system is desirable. Recent experimental work by Abe *et al.*,<sup>[2]</sup> Okazaki *et al.*,<sup>[3]</sup> and Yukawa and co-workers,<sup>[4,43]</sup> on phase equilibria in the Fe-Cr-Mn system was mainly directed toward the determination of the fcc/fcc+sigma phase boundaries at 923 K, which was thought to be the maximum temperature for the alloys to reach in fusion reactors.<sup>[43]</sup> In all of the previous experimental works, the specimens, after solution treatment, were cold-rolled by about 50 pct at room temperature and subsequently aged at 923 K and/or at other temperatures. The work by Abe *et al.*<sup>[2]</sup> showed that an Fe-10Cr-30Mn alloy yielded fcc+sigma two-phase equilibrium after 10 hours at 923 K. This was different from the old data by Schafmeister and Ergang<sup>[6]</sup> where the alloy was located in the single fcc region. Okazaki *et al.*,<sup>[3]</sup> using high-purity materials (99.98 wt pct level), investigated the phase equilibria between fcc and sigma phase. Aging time was 1000 hours, and the experimental results showed that the fcc/fcc+sigma phase boundary of the Fe-Cr-Mn system at 923 K should be located between 10 and 12 wt pct Cr at 15 wt pct Mn. However, Yukawa *et al.*<sup>[4]</sup> reported rather different results under the same conditions. By them, the fcc/fcc+sigma phase boundary had to be located between 4 and 6 wt pct Cr at the same temperature and the same manganese content. The extent of cold rolling before aging was the same at 50 pct, while the aging time was also the same at 1000 hours. The details of their experimental work were published again.<sup>[43]</sup> The only apparent difference was the purity level of materials used by both authors (99.9 wt pct level in Yukawa *et al.*'s work vs. 99.98 wt pct in Okazaki *et al.*'s).

Experimental information on the liquidus surface and liquid/bcc equilibria is also available from the work by Kundrat.<sup>[44]</sup> Using materials of 99.9 wt pct purity level, he measured the liquidus points of several Fe-Cr-Mn ternary alloys by a differential thermal analysis method. He presented a liquidus surface for the Fe-rich part of the Fe-Cr-Mn system in the composition range of up to 24 wt pct Cr and 12 wt pct Mn. The liquid/bcc tie-lines of some alloys in the same composition region were also determined by measuring the chemical composition of each phase in directionally solidified specimens prepared by holding at the liquid+bcc two-phase equilibrium temperature, utilizing high-energy emission spectrography. Besides this, Mukai *et al.*<sup>[45]</sup> investigated the manganese

activity in the Fe-rich dilute liquid alloys at 1570 °C by using a closed chamber method. They reported a value of 0.9 for  $\epsilon_{Mn}^{Cr} (= \partial \ln \gamma_{Mn} / \partial x_{Cr})$  in the composition range of  $x_{Cr} < 0.034$ . This seems to be the only experimental information on thermodynamic properties of the Fe-Cr-Mn ternary alloys.

#### IV. EVALUATION OF MODEL PARAMETERS

The evaluation of the various parameters was made by means of a computer program for the optimization of thermodynamic parameters, PARROT, developed by Jansson.<sup>[46]</sup> The optimization was performed with the selected set of data which will be described in this section, and each piece of information was given a certain weight, reflecting the experimental uncertainty. The weight could be changed until a satisfactory description of most of the selected experimental information was achieved.

For the thermodynamic descriptions of pure iron, those by Fernández Guillermet and Gustafson<sup>[47]</sup> (bcc, fcc, hcp, liquid) and Huang<sup>[12]</sup> ( $\beta$ -Mn,  $\alpha$ -Mn) were accepted. For those of pure chromium, those by Andersson<sup>[48]</sup> (bcc, liquid), Andersson *et al.*<sup>[49]</sup> (fcc, hcp), and Kaufman<sup>[10]</sup> ( $\beta$ -Mn,  $\alpha$ -Mn), and for pure manganese, those by Fernández Guillermet and Huang<sup>[50]</sup> (bcc, fcc, liquid,  $\beta$ -Mn,  $\alpha$ -Mn) and Saunders *et al.*<sup>[51]</sup> (hcp) were used in the present study. For the thermodynamic descriptions of the Fe-Cr and Fe-Mn systems, those by Andersson<sup>[11]</sup> and Huang<sup>[12]</sup> were used, respectively.

##### A. The Cr-Mn Binary System

The solution phases, liquid, bcc, fcc,  $\beta$ -Mn,  $\alpha$ -Mn, and the sigma phase, and the intermediate compound  $\alpha'$  were considered in the present study on the thermodynamic evaluation of the Cr-Mn system. Therefore, the  $L$  parameters of the liquid, bcc, fcc,  $\beta$ -Mn, and  $\alpha$ -Mn the  $G$  (Gibbs energy of formation) and  $L$  parameters of the sigma phase, and the  $G$  parameter of the  $\alpha'$  phase were the thermodynamic model parameters to be evaluated. For those phases where magnetic ordering is reported, model parameters for the Curie or Néel temperatures ( $T_C$ ) and for the average magnetic moment per atom ( $\beta$ ) also should be evaluated.

First, magnetic properties of individual phases in the Cr-Mn binary system were considered. The Néel temperature data reported by several authors,<sup>[8,33-36]</sup> which show reasonable agreement with each other, could have been used to optimize the Néel temperature parameters for the bcc phase as a function of composition. However, the Néel temperature data for the bcc phase were very difficult to fit due to an abrupt increase at low Mn content. High powers in the polynomial for the concentration dependence were necessary to obtain satisfactory fitting. Further, to avoid an unreasonable peak in the calculated Néel temperature in the Mn-rich region where no experimental information is available, only even powers were used in the polynomial though it might be unusual. Then parameters for the average magnetic moment per atom of this phase were optimized using enthalpy data of magnetic ordering by Pepperhoff and Ettwig.<sup>[35]</sup> In their article, the enthalpy values were presented in graphic form as specific heat vs temperature.

From this, a rough estimate of the enthalpy values at each alloy composition was made. This, combined with the fact that the enthalpy of magnetic ordering yields a maximum value of approximately 500 J/mol at 8.1 at pct Mn, was included in the optimization procedure with the highest weight. There was no experimental information on significant magnetic ordering in other phases.

The interaction parameter of the bcc phase,  $L_{Cr,Mn}^{bcc}$ , could be optimized using manganese activity data for this phase. However, as mentioned in Section III, there was severe disagreement between experimental data by individual investigators.<sup>[27-32]</sup> It seemed meaningless to include all the data in the optimization procedure. Therefore, some selection had to be made first. It was fortunate that all the experimental data by Jacob,<sup>[28]</sup> Ranganathan and Hajra,<sup>[29,30]</sup> and Zaitsev *et al.*,<sup>[32]</sup> who measured the manganese activity at several temperatures, showed an agreement in having negative values of the excess entropy of mixing though the absolute values were different from authors to authors. By this, the manganese activity should increase with increasing temperature at constant composition. The data reported by Jacob showed the lowest values even though the experiment was carried out at the highest temperature among various investigations. Thus, his data were excluded from the present optimization. The data by Eremenko *et al.*<sup>[27]</sup> and Lukashenko and Sidorko<sup>[31]</sup> were criticized by themselves as resulting from an inadequate method for measuring manganese activities in the Cr-rich region. Therefore, they were discarded also.

The experimental data by Ranganathan and Hajra<sup>[29,30]</sup> and Zaitsev *et al.*<sup>[32]</sup> disagreed significantly and thus could not be included together in the optimization procedure. When the interaction parameter was optimized using only Ranganathan and Hajra's data, the resultant excess entropy of mixing was too negative (over  $-20$  J/mol·K at 50 at. pct Mn), which seemed unusual; but when Zaitsev *et al.*'s data were used, it yielded reasonable values for both the enthalpy and excess entropy of mixing. Agreement between the currently accepted phase diagram of the Cr-Mn system<sup>[9]</sup> and the phase boundaries computed by Zaitsev *et al.* using their own thermodynamic data led to the decision to accept only Zaitsev *et al.*'s data for optimization of the  $L$  parameter of the Cr-Mn bcc phase.

The next phase to be evaluated was the liquid. The liquidus/solidus data by Carlile *et al.*<sup>[19]</sup> and Hellawell and Hume-Rothery,<sup>[25]</sup> and the liquidus data by Greenaway *et al.*<sup>[22]</sup> could be used for optimization of the interaction parameter of the liquid phase,  $L_{Cr,Mn}^{LIQUID}$ . However, the experimentally determined melting point of chromium by Carlile *et al.* and Greenaway *et al.* was 1845 °C and 1835 °C, respectively, which is lower by 62 °C and 72 °C than the currently accepted value of 1907 °C.<sup>[20]</sup> It would be meaningless to use binary information which is in conflict with the unary part in order to optimize binary interaction parameters. In the present study, the Cr-Mn binary liquidus/solidus points by Carlile *et al.* and Greenaway *et al.* were shifted so that their values for the melting points of pure Cr lie on the currently accepted value. That is, 62  $X_{Cr}$  and 72  $X_{Cr}$  were added

to their temperature values, respectively. These temperature values were then included in the optimization procedure. The liquidus/solidus data by Hellawell and Hume-Rothery were confined to the Mn-rich region and yielded 1244 °C to 1245 °C as the melting point of pure Mn, which is close to the currently accepted value, 1246 °C.<sup>[20]</sup> Therefore, no correction was made for their data assuming that the discrepancy from the different temperature scale (IPTS-48) was less than the experimental error in measuring temperature.

The fcc and  $\beta$ -Mn phases were to be evaluated considering the phase equilibria among bcc, fcc, and  $\beta$ -Mn phases in the Mn-rich region of the Cr-Mn phase diagram. As already mentioned, there was considerable disagreement between the recent experimental information by Hellawell and Hume-Rothery<sup>[25]</sup> and Lugscheider and Ettmayer.<sup>[26]</sup> According to Hellawell and Hume-Rothery, the fcc phase should be stable only in the narrow composition range of 99 to 100 at. pct Mn. Then a peritectoid reaction of  $bcc+fcc\rightarrow\beta$ -Mn should occur and there should be a  $bcc+\beta$ -Mn two-phase equilibrium region with decreasing manganese content until a eutectoid reaction of  $bcc\rightarrow\sigma+\beta$ -Mn occurs at a  $\beta$ -Mn composition of about 91 at pct Mn. The  $bcc+\beta$ -Mn two-phase region was rather similar with that of Carlile *et al.* if the fcc phase region in their phase diagram is replaced with a bcc phase region. However, according to Lugscheider and Ettmayer, there should be no  $bcc+\beta$ -Mn two-phase region. Instead, there should be  $bcc+fcc$  and  $fcc+\beta$ -Mn two-phase regions separated by a fcc one-phase region which extends to the composition of about 93 at pct Mn to yield  $bcc\rightarrow\sigma+fcc$  and  $fcc\rightarrow\sigma+\beta$ -Mn eutectoid reactions. Both sets of experimental information were included in the optimization procedure, and the optimization of  $L$  parameters of the fcc and  $\beta$ -Mn phases was performed using one set of experimental data at each time. It was found that the experimental phase equilibria by Lugscheider and Ettmayer were very difficult to reproduce by calculation, while those by Hellawell and Hume-Rothery were easily reproduced with reasonable values of  $L$  parameters for the fcc and  $\beta$ -Mn phases. Considering this and the fact that the experimental data by Hellawell and Hume-Rothery on phase equilibria in other binary systems, which were published in the same article together with those in the Cr-Mn system, have been widely used and accepted as reliable information, a final decision was made to accept Hellawell and Hume-Rothery's data concerning the stability region of the fcc phase. However, Hellawell and Hume-Rothery's data only were not enough to obtain an acceptable fcc  $L$  parameter, because the two-phase regions that included the fcc phase were too Mn rich and were too narrow. In such cases, a small error in measuring the temperature or composition of phase boundaries can yield large scatter in the optimized parameter values.<sup>[52]</sup> To diminish this kind of error, the data on the fcc/bcc equilibria in the Fe-Cr-Mn ternary system by Kirchner and Uhrenius<sup>[7]</sup> were also included in the optimization procedure for the evaluation of the Cr-Mn binary  $L$  parameters of the fcc and  $\beta$ -Mn phases.

The next phase to be evaluated was the sigma phase. From the work by Kaufman,<sup>[10]</sup> it seems impossible to reproduce the abrupt change in slope of the  $bcc/bcc+\sigma$  phase boundary at 998 °C successfully when

describing sigma as one phase with an order-disorder transition. Since most experimental investigations of phase equilibria in this region show good agreement, this change could not be ignored only for the sake of simplicity. The only way to solve this difficulty was to use two models for this phase as if it were two different phases with similar structure, one above the transformation temperature around 998 °C and the other below that temperature. Actually, Wachtel and Bartelt<sup>[8]</sup> reported another transformation in the sigma phase at about 800 °C and also in the  $\alpha'$  phase at about 600 °C; but additional experimental data on the details of these transformations are not available. Thus, the second  $\alpha'$  phase and the second transformation in the sigma phase<sup>[8]</sup> were not considered in the present study. The  $\alpha'$  phase was treated as one stoichiometric compound with composition of  $\text{Cr}_3\text{Mn}_5$  considering Wachtel and Bartelt's experimental data<sup>[8]</sup> on the stability region of this phase.

As mentioned earlier, the phase below the transformation temperature around 998 °C was regarded as ordinary  $\sigma$  phase, because  $\sigma$  phase usually occurs at low temperature in other binary systems. The phase above the transformation temperature was regarded as another  $\sigma$  phase with similar structure but different thermodynamic properties and is denoted  $h_\sigma$  in the present study. The experimental data by Carlile *et al.*<sup>[19]</sup> on the two peritectic reactions among the liquid, bcc, and  $h_\sigma$  phases and on the invariant reaction among the bcc,  $h_\sigma$ , and  $\beta$ -Mn phases and those by various authors<sup>[18,23,24]</sup> on the invariant reaction at about 998 °C between the bcc,  $h_\sigma$ , and  $\sigma$  phases were included in the optimization procedure.

The model parameters of the  $\sigma$  and  $\alpha$ -Mn phases were optimized simultaneously in one optimization procedure together with those of the  $h_\sigma$  phase. The experimental data included those on the bcc/bcc+ $\sigma$  phase boundary below 998 °C by Pearson and Hume-Rothery<sup>[24]</sup> and Wachtel and Bartelt<sup>[8]</sup> and those on the invariant reaction among the  $\sigma$ ,  $\alpha$ -Mn, and  $\beta$ -Mn phases by Carlile *et al.*<sup>[19]</sup>

Lugscheider and Ettmayer<sup>[26]</sup> reported the  $\sigma + \beta - \text{Mn} \rightarrow \alpha - \text{Mn}$  invariant reaction temperature as 900 °C, which is higher than Carlile *et al.*<sup>[19]</sup> or Zwicker<sup>[23]</sup> by 100 °C. However, this value (900 °C) was ignored in the present study, because it made the  $\alpha$ -Mn phase too stable in another region of the calculated phase diagram.

To diminish the possible error in evaluating the temperature dependencies of model parameters of the  $\sigma$  and  $\alpha$ -Mn phases, some artificial data points were included in the optimization procedure so that the  $\sigma + \alpha - \text{Mn}$  two-phase region would lie between 77 and 92 at. pct Mn at 500 °C, in accordance with data points by Carlile *et al.*<sup>[19]</sup> Pearson and Hume-Rothery,<sup>[24]</sup> and Wachtel and Bartelt<sup>[8]</sup> on the single-phase/two-phase region at low temperatures. Finally, the  $G$  parameter of the  $\alpha'$  phase was evaluated from the bcc +  $\sigma \rightarrow \alpha'$  invariant reaction temperature data by Wachtel and Bartelt.<sup>[8]</sup> Its temperature dependence could be estimated considering the hypothetical phase boundary, bcc/bcc +  $\alpha'$ , proposed by Wachtel and Bartelt and the experimental data points on single-phase/two-phase region at 600 °C by Zwicker.<sup>[23]</sup>

## B. The Fe-Cr-Mn Ternary System

The possible presence of other phases in this system has been reported by Fritscher and Hammelrath<sup>[53]</sup> ( $Y$

phase) and Okazaki *et al.*<sup>[3]</sup> ( $\chi$ ). However, these investigations were not followed by subsequent experimental studies, and thus, no more ternary phase was considered in the present evaluation of the Fe-Cr-Mn system; but it should be noted that the results by Okazaki *et al.* indicate that the  $\chi$  phase may be in a metastable state that is rather close to the stable state.

No experimental information was available on magnetic properties of Fe-Cr-Mn alloys. Therefore descriptions of the Curie or Néel temperatures and magnetic moments of the binary alloys were simply combined to give those for the Fe-Cr-Mn ternary. No further attention was paid to the  $\alpha'$  phase, because it was treated as a stoichiometric binary compound. Due to a lack of relevant experimental information, the thermodynamic parameters  $L_{\text{Fe,Cr}}$  and  $L_{\text{Fe,Cr,Mn}}$  of the ternary  $\beta$ -Mn and  $\alpha$ -Mn phases could not be evaluated and were given the value, zero, arbitrarily.

Now the remaining phases to be evaluated are the bcc, fcc,  $\sigma$ ,  $h_\sigma$ , and liquid phases. Liquid is the only phase in the Fe-Cr-Mn ternary system where thermodynamic data is available. The experimental value of 0.9<sup>[45]</sup> for  $\epsilon_{\text{Mn}}^{\text{Cr}} (= \partial \ln \gamma_{\text{Mn}} / \partial x_{\text{Cr}})$  in Fe-rich dilute liquid alloys could be well reproduced by giving a value of 2378 J/mol to the ternary  $L$  parameter of the liquid phase. Then, Kundrat's data<sup>[44]</sup> on the liquidus surface and liquid/bcc tie-lines were used to evaluate the temperature-independent ternary interaction parameter of the bcc phase. The bcc/fcc equilibrium data between 750 °C and 950 °C by Kirchner and Uhrenius<sup>[7]</sup> could be well reproduced by giving the same value to the ternary  $L$  parameter of the fcc phase as for the bcc. However, Okazaki *et al.*'s data on the same equilibria at higher temperatures (1000 °C to 1200 °C) showed that the fcc phase should be more stable than the bcc at high temperature. Therefore, in the final step of the optimization, a ternary interaction parameter of a linearly temperature-dependent form was introduced for the fcc phase. Here, it should be noted that the interaction parameters of the binary Fe-Cr liquid phase were slightly modified in order to obtain better agreement around the Fe-20 pct Cr ternary composition between the calculated and experimental liquidus and the bcc/liquid tie-lines. By this modification, it became possible also to obtain better agreement for the Fe-rich liquidus of the Fe-Cr-C and Fe-Cr-Ni systems than in the previous assessments by Lee<sup>[54]</sup> and Hillert and Qiu.<sup>[55]</sup> The details of this modification were written separately.<sup>[56]</sup>

All of the experimental information on the Fe-Cr-Mn system reviewed in Section A is mainly on the Fe-rich part. No reliable information is available for the remaining composition range. A probable question is whether the Fe-Cr  $\sigma$  phase and the Cr-Mn  $\sigma$  phase will form a continuous solid solution in the temperature range where each  $\sigma$  phase is stable in a corresponding binary side. The 700 °C isothermal section proposed by Fritscher and Hammelrath<sup>[53]</sup> shows a separation of each  $\sigma$  phase by an unidentified phase ( $Y$ ); but when considering the vertical sections by Grigor'ev and Gruzdeva<sup>[39]</sup> and microstructure studies on the Fe-15 pct Cr-40 pct Mn and Fe-14 pct Cr-29 pct Mn alloys at 650 °C by Shevdov and Pavlenko,<sup>[57]</sup> it can be concluded that a continuous transition between each  $\sigma$  phase is possible. Therefore,

when compiling hypothetical isothermal sections covering the whole composition range, Potucek<sup>[58]</sup> and Rivlin and Raynor<sup>[59]</sup> assumed a continuous solid solution between the two  $\sigma$  phases. Recent experimental data on the 650 °C isothermal section by Murata *et al.*<sup>[43]</sup> and work by Lemkey *et al.*,<sup>[60]</sup> who detected the  $\sigma$  phase and measured lattice parameters of it in ternary alloys with compositions corresponding to  $\text{Fe}_2\text{Cr}_5\text{Mn}_9$ ,  $\text{Fe}_4\text{Cr}_6\text{Mn}_6$ , and  $\text{Fe}_6\text{Cr}_7\text{Mn}_3$  after annealing at 700 °C, confirm the preceding assumption.

However, there is still a difficulty in evaluating thermodynamic properties of the two different sigma phases, the  $h_\sigma$  and ordinary  $\sigma$  phase. The difficulty comes from the fact that there is no experimental information available on the phase transformation of the ternary sigma phase even though it is well defined in the Cr-Mn binary side. The three-sublattice model adapted to describe the ternary sigma phase contains six  $G$  parameters as well as several  $L$  parameters. Two of these  $G$  parameters are for the Fe-Cr-Mn ternary, two are for the Fe-Cr binary, and two are for the Cr-Mn binary. Among the six  $G$  parameters, the two ternary ones must be newly evaluated in the case of ordinary  $\sigma$  phase. However, in the case of the  $h_\sigma$  phase, the number of  $G$  parameters to be newly evaluated increases to four because the binary Fe-Cr parameters for the hypothetical  $h_\sigma$  phase should also be evaluated. Unfortunately, the experimental information was not sufficient to evaluate all these parameters with confidence. Some assumptions and approximations had to be made to decrease the number of adjustable parameters in order to diminish the probable error that results from evaluating too many parameters using incomplete experimental information. First, it was assumed that the model parameters of the Fe-Cr  $h_\sigma$  phase were the same as those of the Fe-Cr  $\sigma$  phase. Second, the interaction between Cr and Mn atoms in the third sublattice of the ternary sigma phase was assumed to be the same as that of the binary Cr-Mn sigma phase, yielding the relation  $L_{\text{Mn:Cr:Cr:Mn}}^{\text{SIGMA}} = L_{\text{Fe:Cr:Cr:Mn}}^{\text{SIGMA}}$ . Third, the ternary  $\Delta^\circ G$  parameters (Eq. [5]) of the sigma phase,  $\Delta^\circ G_{\text{Fe:Cr:Mn}}^{\text{SIGMA}}$  and  $\Delta^\circ G_{\text{Mn:Cr:Fe}}^{\text{SIGMA}}$ , were approximated as the weighted averages of related binary parameters,  $\Delta^\circ G_{\text{Fe:Cr:Fe}}^{\text{SIGMA}}$  and  $\Delta^\circ G_{\text{Mn:Cr:Mn}}^{\text{SIGMA}}$ , with a temperature-independent correction term. This approximation yields the following relations:

$$\Delta^\circ G_{\text{Fe:Cr:Mn}}^{\text{SIGMA}} = \frac{8}{26} \Delta^\circ G_{\text{Fe:Cr:Fe}}^{\text{SIGMA}} + \frac{18}{26} \Delta^\circ G_{\text{Mn:Cr:Mn}}^{\text{SIGMA}} + \Delta^{\text{cor}} G_{\text{Fe:Cr:Mn}}^{\text{SIGMA}} \quad [6]$$

$$\Delta^\circ G_{\text{Mn:Cr:Fe}}^{\text{SIGMA}} = \frac{18}{26} \Delta^\circ G_{\text{Fe:Cr:Fe}}^{\text{SIGMA}} + \frac{8}{26} \Delta^\circ G_{\text{Mn:Cr:Mn}}^{\text{SIGMA}} + \Delta^{\text{cor}} G_{\text{Mn:Cr:Fe}}^{\text{SIGMA}} \quad [7]$$

Finally, the correction terms,  $\Delta^{\text{cor}} G_{\text{Fe:Cr:Mn}}^{\text{SIGMA}}$  and  $\Delta^{\text{cor}} G_{\text{Mn:Cr:Fe}}^{\text{SIGMA}}$ , of both sigma phases were assumed to have the same values, respectively. This assumption gives the relations  $\Delta^{\text{cor}} G_{\text{Fe:Cr:Mn}}^{\text{SIGMA}} = \Delta^{\text{cor}} G_{\text{Fe:Cr:Mn}}^{\sigma}$  and  $\Delta^{\text{cor}} G_{\text{Mn:Cr:Fe}}^{\text{SIGMA}} = \Delta^{\text{cor}} G_{\text{Mn:Cr:Fe}}^{\sigma}$  and means that the addition of Fe atoms to

the Cr-Mn binary alloys gives the same effects on the thermodynamic properties of both sigma phases. Using the preceding four assumptions or approximation, the number of parameters was decreased to only two, the two correction terms. An optimization to evaluate the correction terms was performed by including all experimental information which was reviewed in Section III. Only one correction term  $\Delta^{\text{cor}} G_{\text{Mn:Cr:Fe}}^{\text{SIGMA}}$  was needed to obtain reasonable agreement with experimental data over the whole temperature range investigated.  $\Delta^{\text{cor}} G_{\text{Fe:Cr:Mn}}^{\text{SIGMA}}$  was thus put to zero.

Although the hcp phase does not appear in the Fe-Cr-Mn ternary system, it appears in the Mn-C binary system. Therefore, it is necessary to evaluate parameters for the metastable hcp phase in this ternary system in order to extend the thermodynamic assessment to the Fe-Cr-Mn-C quaternary. In the assessment of the Fe-Mn system,<sup>[12]</sup> Huang has evaluated parameters for the  $\epsilon$ (hcp) phase based on martensitic transformation temperatures. In her assessment, the calculated metastable equilibrium boundaries were in rather good agreement with experimentally reported  $A_s^{\epsilon \rightarrow \gamma}$  and  $M_s^{\gamma \rightarrow \epsilon}$  temperatures. The effects of Cr additions on the  $A_s^{\epsilon \rightarrow \gamma}$  and  $M_s^{\gamma \rightarrow \epsilon}$  temperatures in the Fe-rich Fe-Cr-Mn alloys were investigated by Georgieva *et al.*,<sup>[61]</sup> who reported that addition of 10 wt pct Cr in the Fe-14, 18, and 22 wt pct Mn alloys decreased the  $A_s^{\epsilon \rightarrow \gamma}$  temperature by about 45 °C to 60 °C. An attempt was made to estimate parameters for the hcp Fe-Cr-Mn ternary phase based on the Fe-Mn<sup>[12]</sup> and Fe-Cr<sup>[62]</sup> phases and considering the preceding experimental data.<sup>[61]</sup> In the present study, only the Cr-Mn binary parameter was evaluated, while the ternary parameter was set equal to zero. When giving a value of 60,000 J/mol to  $L_{\text{Cr:Mn}}^{\text{hcp}}$ , the calculated metastable equilibria between the fcc and hcp phases could reproduce the effect of Cr addition on the  $A_s^{\epsilon \rightarrow \gamma}$  temperature. However, it should be said that the  $A_s^{\epsilon \rightarrow \gamma}$  temperature does not represent the metastable equilibrium between the two phases. Therefore, the present evaluation of the Cr-Mn binary interaction parameter of the hcp phase,  $L_{\text{Cr:Mn}}^{\text{hcp}}$ , is only an approximation. A more accurate value should be proposed later from an assessment of a higher order system including chromium and manganese.

The thermodynamic parameters of the Fe-Cr-Mn system are listed in Table I. The parameters evaluated in the present work are denoted with an asterisk “\*”.

## V. RESULTS AND DISCUSSION

All calculations of phase equilibria were carried out by using a computer program, Thermo-Calc, developed by Sundman *et al.*<sup>[63]</sup> The calculated phase diagram of the Cr-Mn system is shown in Figure 1. Figure 2 shows the same diagram in comparison with experimental data. The Mn-rich region and central part of the calculated phase diagram are presented in more detail in Figures 3 and 4, respectively, in comparison with other relevant experimental data. Though there is little discrepancy among various experimental data sets, the calculated phase diagram shows satisfactory agreements with the scattered experimental data points.

As shown in Figure 4, the experimental data by Pearson

**Table I. The Thermodynamic Properties of the Fe-Cr-Mn System (All Values in SI Units for One Formula Unit)**

The magnetic contribution to Gibbs energy is described by  ${}^mG_m = RT \ln (\beta + 1)f(\tau)$ ,  $\tau = T/T_c$

$$\text{for } \tau < 1: f(\tau) = 1 - \left[ \frac{79\tau^{-1}}{140p} + \frac{474}{497} \left( \frac{1}{p} - 1 \right) \left( \frac{\tau^3}{6} + \frac{\tau^9}{135} + \frac{\tau^{15}}{600} \right) \right] / A$$

$$\text{for } \tau > 1: f(\tau) = - \left( \frac{\tau^{-5}}{10} + \frac{\tau^{-15}}{315} + \frac{\tau^{-25}}{1500} \right) / A$$

$$\text{where } A = \frac{518}{1125} + \frac{11,692}{15,975} \left( \frac{1}{p} - 1 \right) \text{ and } p \text{ depends on the structure.}$$

The bcc, fcc, hcp, and  $\alpha$ -Mn phases have magnetic contributions.  $p$  is 0.4 for bcc and 0.28 for fcc, hcp, and  $\alpha$ -Mn.  ${}^\circ G^\phi$  below is the Gibbs energy of the  $\phi$  phase in a nonmagnetic state.

### Liquid

$$298.15 < T < 1811.00$$

$${}^\circ G_{\text{Fe}}^{\text{LIQUID}} - H_{\text{Fe}}^{\text{SER}} = \text{GHSERFE} + 12,040.17 - 6.55843T - 3.6751551 \cdot 10^{-21}T^7 \quad 1811.00 < T < 6000.00$$

$${}^\circ G_{\text{Fe}}^{\text{LIQUID}} - H_{\text{Fe}}^{\text{SER}} = \text{GHSERFE} + 14,544.751 - 8.01055T - 2.29603 \cdot 10^{31}T^{-9} \quad 298.15 < T < 2180.00$$

$${}^\circ G_{\text{Cr}}^{\text{LIQUID}} - H_{\text{Cr}}^{\text{SER}} = \text{GHSERCR} + 24,339.955 - 11.420225T - 2.37615 \cdot 10^{-21}T^7 \quad 2180.00 < T < 6000.00$$

$${}^\circ G_{\text{Cr}}^{\text{LIQUID}} - H_{\text{Cr}}^{\text{SER}} = \text{GHSERCR} + 18,409.36 - 8.563683T - 2.88526 \cdot 10^{32}T^{-9} \quad 298.15 < T < 1519.00$$

$${}^\circ G_{\text{Mn}}^{\text{LIQUID}} - H_{\text{Mn}}^{\text{SER}} = \text{GHSERMN} + 17,859.91 - 12.6208T - 4.41929 \cdot 10^{-21}T^7 \quad 1519.00 < T < 2000.00$$

$${}^\circ G_{\text{Mn}}^{\text{LIQUID}} - H_{\text{Mn}}^{\text{SER}} = \text{GHSERMN} + 18,739.51 - 13.2288T - 1.656847 \cdot 10^{30}T^{-9}$$

$$*L_{\text{Fe,Cr}}^{\text{LIQUID}} = -17,737 + 7.996546T + 1331 (y_{\text{Fe}} - y_{\text{Cr}})$$

$$L_{\text{Fe,Mn}}^{\text{LIQUID}} = -3950 + 0.489T + 1145 (y_{\text{Fe}} - y_{\text{Mn}})$$

$$*L_{\text{Cr,Mn}}^{\text{LIQUID}} = -15009 + 13.6587T + (504 + 0.9479T) (y_{\text{Cr}} - y_{\text{Mn}})$$

$$*L_{\text{Fe,Cr,Mn}}^{\text{LIQUID}} = +2378$$

### Bcc

$${}^\circ G_{\text{Fe}}^{\text{bcc}} - H_{\text{Fe}}^{\text{SER}} = +\text{GHSERFE}$$

$${}^\circ G_{\text{Cr}}^{\text{bcc}} - H_{\text{Cr}}^{\text{SER}} = +\text{GHSERCR}$$

$${}^\circ G_{\text{Mn}}^{\text{bcc}} - H_{\text{Mn}}^{\text{SER}} = +\text{GMNBCC}$$

$$L_{\text{Fe,Cr}}^{\text{bcc}} = +20,500 - 9.68T$$

$$L_{\text{Fe,Mn}}^{\text{bcc}} = -2759 + 1.237T$$

$$*L_{\text{Cr,Mn}}^{\text{bcc}} = -20,328 + 18.7339T + (-9162 + 4.4183T)(y_{\text{Cr}} - y_{\text{Mn}})$$

$$*L_{\text{Fe,Cr,Mn}}^{\text{bcc}} = -5996$$

$$*T_{\text{C}}^{\text{bcc}} = +1043y_{\text{Fe}} - 311.5y_{\text{Cr}} - 580y_{\text{Mn}} + y_{\text{Fe}}y_{\text{Cr}}[1650 - 550(y_{\text{Fe}} - y_{\text{Cr}})] \\ + y_{\text{Fe}}y_{\text{Mn}}[123] + y_{\text{Cr}}y_{\text{Mn}}[-1325 - 1133(y_{\text{Cr}} - y_{\text{Mn}})^2 - 10,294(y_{\text{Cr}} - y_{\text{Mn}})^4 \\ + 26,706(y_{\text{Cr}} - y_{\text{Mn}})^6 - 28,117(y_{\text{Cr}} - y_{\text{Mn}})^8]$$

$$*\beta^{\text{BCC}} = +2.22y_{\text{Fe}} - 0.008y_{\text{Cr}} - 0.27y_{\text{Mn}} - 0.85y_{\text{Fe}}y_{\text{Cr}} \\ + y_{\text{Cr}}y_{\text{Mn}}[0.48643 - 0.72035(y_{\text{Cr}} - y_{\text{Mn}})^2 - 1.93265(y_{\text{Cr}} - y_{\text{Mn}})^4]$$

### fcc

$${}^\circ G_{\text{Fe}}^{\text{fcc}} - H_{\text{Fe}}^{\text{SER}} = +\text{GF EFCC}$$

$${}^\circ G_{\text{Cr}}^{\text{fcc}} - H_{\text{Cr}}^{\text{SER}} = +\text{GCRFCC}$$

$${}^\circ G_{\text{Mn}}^{\text{fcc}} - H_{\text{Mn}}^{\text{SER}} = +\text{GMNFCC}$$

$$L_{\text{Fe,Cr}}^{\text{fcc}} = +10,833 - 7.477T - 1410 (y_{\text{Fe}} - y_{\text{Cr}})$$

$$L_{\text{Fe,Mn}}^{\text{fcc}} = -7762 + 3.865T - 259 (y_{\text{Fe}} - y_{\text{Mn}})$$

$$*L_{\text{Cr,Mn}}^{\text{fcc}} = -19,088 + 17.5423T$$

$$*L_{\text{Fe,Cr,Mn}}^{\text{fcc}} = +6715 - 10.3933T$$

$$T_{\text{C}}^{\text{fcc}} = -201y_{\text{Fe}} - 1109y_{\text{Cr}} - 1620y_{\text{Mn}} + y_{\text{Fe}}y_{\text{Mn}}[-2282 - 2068(y_{\text{Fe}} - y_{\text{Mn}})]$$

$$\beta^{\text{fcc}} = -2.1y_{\text{Fe}} - 2.46y_{\text{Cr}} - 1.86y_{\text{Mn}}$$

### $\beta$ -Mn

$${}^\circ G_{\text{Fe}}^{\beta\text{-Mn}} - H_{\text{Fe}}^{\text{SER}} = +\text{GHSERFE} + 3745$$

$${}^\circ G_{\text{Cr}}^{\beta\text{-Mn}} - H_{\text{Cr}}^{\text{SER}} = +\text{GHSERCR} + 15,899 + 0.6276T$$

$$298.15 < T < 1519.00$$

$${}^\circ G_{\text{Mn}}^{\beta\text{-Mn}} - H_{\text{Mn}}^{\text{SER}} = -5800.4 + 135.995T - 24.8785T \ln T - 0.00583359T^2 + 70,269T^{-1}$$

$$1519.00 < T < 2000.00$$

$${}^\circ G_{\text{Mn}}^{\beta\text{-Mn}} - H_{\text{Mn}}^{\text{SER}} = -28,290.76 + 311.2933T - 48T \ln T + 3.96757 \cdot 10^{30}T^{-9}$$

$$L_{\text{Fe,Mn}}^{\beta\text{-Mn}} = -11,518 + 2.819T$$

$$*L_{\text{Cr,Mn}}^{\beta\text{-Mn}} = -31,260 + 16.4919T$$



**Table I Cont. The Thermodynamic Properties of the Fe-Cr-Mn System (All Values in SI Units for One Formula Unit)**

**$\alpha$ -Mn**

$$\begin{aligned} {}^{\circ}G_{\text{Fe}}^{\alpha\text{-Mn}} - H_{\text{Fe}}^{\text{SER}} &= +\text{GHSErFE} + 4745 \\ {}^{\circ}G_{\text{Cr}}^{\alpha\text{-Mn}} - H_{\text{Cr}}^{\text{SER}} &= +\text{GHSErCR} + 11,087 + 2.7196T \\ {}^{\circ}G_{\text{Mn}}^{\alpha\text{-Mn}} - H_{\text{Mn}}^{\text{SER}} &= +\text{GHSErMN} \\ L_{\text{Fe,Mn}}^{\alpha\text{-Mn}} &= -10,184 \\ *L_{\text{Cr,Mn}}^{\alpha\text{-Mn}} &= -38,349 + 22.6925T \\ T_{\text{C}}^{\alpha\text{-Mn}} &= -285y_{\text{Mn}} \\ \beta^{\alpha\text{-Mn}} &= -0.66y_{\text{Mn}} \end{aligned}$$

**HCP**

$$\begin{aligned} {}^{\circ}G_{\text{Fe}}^{\text{hcp}} - H_{\text{Fe}}^{\text{SER}} &= +\text{GFEFCC} - 2243.4 + 4.3095T \\ {}^{\circ}G_{\text{Cr}}^{\text{hcp}} - H_{\text{Cr}}^{\text{SER}} &= +\text{GHSErCR} + 4438 \\ {}^{\circ}G_{\text{Mn}}^{\text{hcp}} - H_{\text{Mn}}^{\text{SER}} &= +\text{GMNFCC} - 1000 + 1.123T \\ L_{\text{Fe,Cr}}^{\text{hcp}} &= +10,833 - 7.477T \\ L_{\text{Fe,Mn}}^{\text{hcp}} &= -5582 + 3.865T + 273(y_{\text{Fe}} - y_{\text{Mn}}) \\ *L_{\text{Cr,Mn}}^{\text{hcp}} &= +60,000 \\ T_{\text{C}}^{\text{hcp}} &= -1109y_{\text{Cr}} - 1620y_{\text{Mn}} \\ \beta^{\text{hcp}} &= -2.46y_{\text{Cr}} - 1.86y_{\text{Mn}} \end{aligned}$$

**$\alpha'$**

2 sublattices, sites 3:5

Constituents Cr:Mn

$${}^{\circ}G_{\text{Cr:Mn}}^{\alpha'} - 3H_{\text{Cr}}^{\text{SER}} - 5H_{\text{Mn}}^{\text{SER}} = +3\text{GHSErCR} + 5\text{GHSErMN} - 72,550 + 21.1732T$$

**$\sigma$**

3 sublattices, sites 8:4:18

Constituents Fe,Mn:Cr: Fe,Cr,Mn

$$\begin{aligned} {}^{\circ}G_{\text{Fe:Cr:Fe}}^{\sigma} - 8H_{\text{Fe}}^{\text{SER}} - 4H_{\text{Cr}}^{\text{SER}} - 18H_{\text{Fe}}^{\text{SER}} &= 8\text{GFEFCC} + 4\text{GHSErCR} + 18\text{GHSErFE} + 117,300 - 95.96T \\ {}^{\circ}G_{\text{Fe:Cr:Cr}}^{\sigma} - 8H_{\text{Fe}}^{\text{SER}} - 4H_{\text{Cr}}^{\text{SER}} - 18H_{\text{Cr}}^{\text{SER}} &= 8\text{GFEFCC} + 22\text{GHSErCR} + 92,300 - 95.96T \\ *{}^{\circ}G_{\text{Mn:Cr:Mn}}^{\sigma} - 8H_{\text{Mn}}^{\text{SER}} - 4H_{\text{Cr}}^{\text{SER}} - 18H_{\text{Mn}}^{\text{SER}} &= 8\text{GMNFCC} + 4\text{GHSErCR} + 18\text{GMNBCC} - 172,946 + 69.0245T \\ *{}^{\circ}G_{\text{Mn:Cr:Cr}}^{\sigma} - 8H_{\text{Mn}}^{\text{SER}} - 4H_{\text{Cr}}^{\text{SER}} - 18H_{\text{Cr}}^{\text{SER}} &= 8\text{GMNFCC} + 22\text{GHSErCR} + 65,859.5 \\ *{}^{\circ}G_{\text{Fe:Cr:Mn}}^{\sigma} - 8H_{\text{Fe}}^{\text{SER}} - 4H_{\text{Cr}}^{\text{SER}} - 18H_{\text{Mn}}^{\text{SER}} &= 8\text{GFEFCC} + 4\text{GHSErCR} + 18\text{GMNBCC} - 83,639.5 + 18.26T \\ *{}^{\circ}G_{\text{Mn:Cr:Fe}}^{\sigma} - 8H_{\text{Mn}}^{\text{SER}} - 4H_{\text{Cr}}^{\text{SER}} - 18H_{\text{Fe}}^{\text{SER}} &= 8\text{GMNFCC} + 4\text{GHSErCR} + 18\text{GHSErFE} - 95,576 - 45.1955T \\ *L_{\text{Fe:Cr:Cr,Mn}}^{\sigma} &= -1,095,771 + 862.0312T \\ *L_{\text{Mn:Cr:Cr,Mn}}^{\sigma} &= -1,095,771 + 862.0312T \end{aligned}$$

**$h_{\sigma}$**

3 sublattices, sites 8:4:18

Constituents Fe,Mn:Cr:Fe,Cr,Mn

$$\begin{aligned} *{}^{\circ}G_{\text{Fe:Cr:Fe}}^{h\text{-}\sigma} - 8H_{\text{Fe}}^{\text{SER}} - 4H_{\text{Cr}}^{\text{SER}} - 18H_{\text{Fe}}^{\text{SER}} &= 8\text{GFEFCC} + 4\text{GHSErCR} + 18\text{GHSErFE} + 117,300 - 95.96T \\ *{}^{\circ}G_{\text{Fe:Cr:Cr}}^{h\text{-}\sigma} - 8H_{\text{Fe}}^{\text{SER}} - 4H_{\text{Cr}}^{\text{SER}} - 18H_{\text{Cr}}^{\text{SER}} &= 8\text{GFEFCC} + 22\text{GHSErCR} + 92,300 - 95.96T \\ *{}^{\circ}G_{\text{Mn:Cr:Mn}}^{h\text{-}\sigma} - 8H_{\text{Mn}}^{\text{SER}} - 4H_{\text{Cr}}^{\text{SER}} - 18H_{\text{Mn}}^{\text{SER}} &= 8\text{GMNFCC} + 4\text{GHSErCR} + 18\text{GMNBCC} - 74,263 - 10.7082T \\ *{}^{\circ}G_{\text{Mn:Cr:Cr}}^{h\text{-}\sigma} - 8H_{\text{Mn}}^{\text{SER}} - 4H_{\text{Cr}}^{\text{SER}} - 18H_{\text{Cr}}^{\text{SER}} &= 8\text{GMNFCC} + 22\text{GHSErCR} - 192,369 + 152.4742T \\ *{}^{\circ}G_{\text{Fe:Cr:Mn}}^{h\text{-}\sigma} - 8H_{\text{Fe}}^{\text{SER}} - 4H_{\text{Cr}}^{\text{SER}} - 18H_{\text{Mn}}^{\text{SER}} &= 8\text{GFEFCC} + 4\text{GHSErCR} + 18\text{GMNBCC} - 15,320.5 - 36.9395T \\ *{}^{\circ}G_{\text{Mn:Cr:Fe}}^{h\text{-}\sigma} - 8H_{\text{Mn}}^{\text{SER}} - 4H_{\text{Cr}}^{\text{SER}} - 18H_{\text{Fe}}^{\text{SER}} &= 8\text{GMNFCC} + 4\text{GHSErCR} + 18\text{GHSErFE} - 65,212 - 69.7287T \\ *L_{\text{Fe:Cr:Cr,Mn}}^{h\text{-}\sigma} &= +90,000 \\ *L_{\text{Mn:Cr:Cr,Mn}}^{h\text{-}\sigma} &= +90,000 \end{aligned}$$

**Symbols**

298.15 < T < 1811.00

$$\text{GHSErFE} = +1225.7 + 124.134T - 23.5143 T \ln T - 0.00439752T^2 - 5.8927 \cdot 10^{-8} T^3 + 77,359T^{-1}$$

1811.00 < T < 6000.00

$$\text{GHSErFE} = -25,383.581 + 299.31255T - 46T \ln T + 2.29603 \cdot 10^{31}T^{-9}$$

298.15 < T < 2180.00

$$\text{GHSErCR} = -8856.94 + 157.48T - 26.908T \ln T + 1.89435 \cdot 10^{-3} T^2 - 1.47721 \cdot 10^{-6}T^3 + 139,250T^{-1}$$

2180.00 < T < 6000.00

$$\text{GHSErCR} = -34,869.344 + 344.18T - 50T \ln T - 2.88526 \cdot 10^{32}T^{-9}$$

298.15 < T < 1519.00

$$\text{GHSErMN} = -8115.28 + 130.059T - 23.4582T \ln T - 0.00734768T^2 + 69827T^{-1}$$

1519.00 < T < 2000.00

**Table I Cont. The Thermodynamic Properties of the Fe-Cr-Mn System (All Values in SI Units for One Formula Unit)**

$$\begin{aligned} \text{GHSERMN} &= -28,733.41 + 312.2648T - 48T \ln T + 1.656847 \cdot 10^{30}T^{-9} \\ 298.15 < T < 1811.00 \\ \text{GFEFCC} &= +\text{GHSEFE} - 1462.4 + 8.282T - 1.15T \ln T + 6.4 \cdot 10^{-4}T^2 \\ 1811.00 < T < 6000.00 \\ \text{GFEFCC} &= -27,098.266 + 300.25256T - 46T \ln T + 2.78854 \cdot 10^{31}T^{-9} \\ \text{GCRFCC} &= +\text{GHSECR} + 7284 + 0.163T \\ 298.15 < T < 1519.00 \\ \text{GMNFCC} &= -3439.3 + 131.884T - 24.5177 T \ln T - 0.006T^2 + 69,600T^{-1} \\ 1519.00 < T < 2000.00 \\ \text{GMNFCC} &= -26,070.1 + 309.6664T - 48T \ln T + 3.86196 \cdot 10^{30}T^{-9} \\ 298.15 < T < 1519.00 \\ \text{GMNBCC} &= -3235.3 + 127.85T - 23.7T \ln T - 0.00744271T^2 + 60,000T^{-1} \\ 1519.00 < T < 2000.00 \\ \text{GMNBCC} &= -23188.83 + 307.7043T - 48T \ln T + 1.265152 \cdot 10^{30}T^{-9} \end{aligned}$$

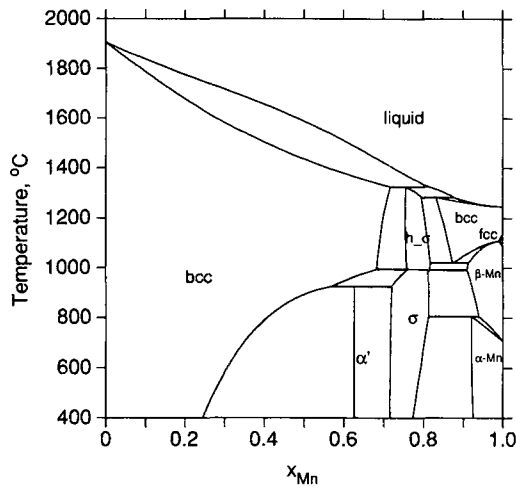


Fig. 1—The calculated phase diagram of the Cr-Mn system.

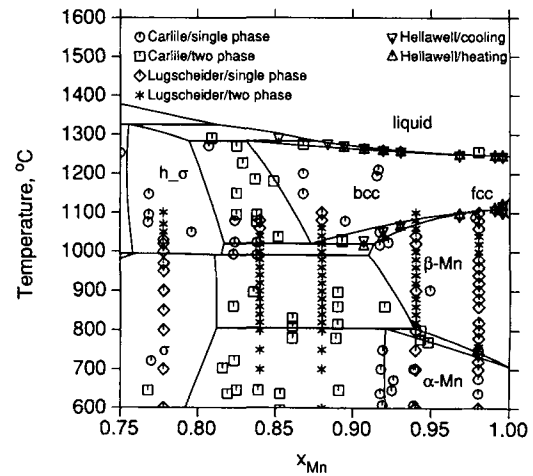


Fig. 3—The calculated phase diagram of the Cr-Mn system in comparison with experimental data (19,25,26).

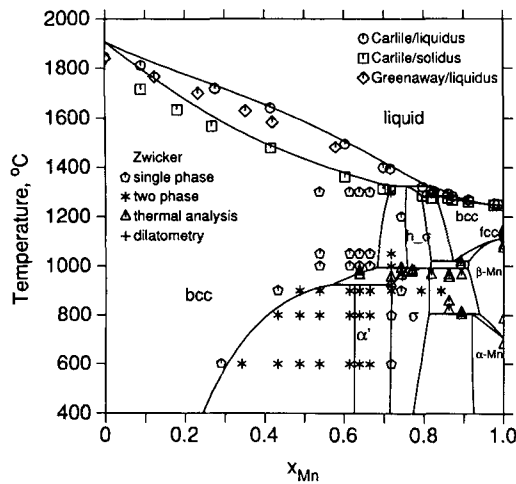


Fig. 2—The calculated phase diagram of the Cr-Mn system in comparison with experimental data (19,22,23).

and Hume-Rothery<sup>[24]</sup> and Wachtel and Bartel<sup>[18]</sup> show higher solubility of manganese in the Cr-rich bcc phase at about 800 °C than in the present calculation. However, when the calculated bcc/bcc+σ phase boundary above 925 °C is extrapolated to lower temperature, it shows good agreement with the preceding experimental data points. Therefore, those experimental data at about

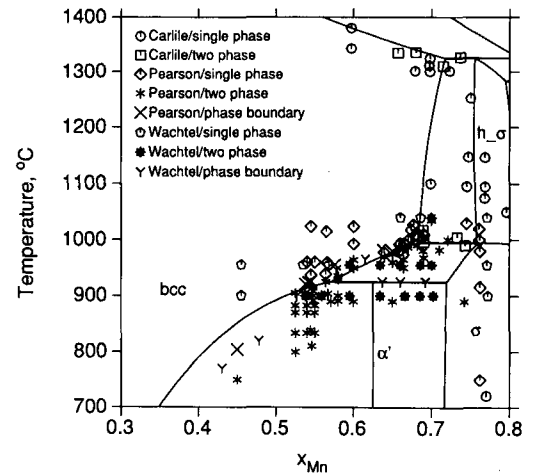


Fig. 4—The calculated phase diagram of the Cr-Mn system in comparison with experimental data (19,24,8).

800 °C can be regarded as for the metastable equilibrium between bcc and  $\sigma$  not for the stable equilibrium between bcc and  $\alpha'$ . The calculated Néel temperatures of the Cr-Mn bcc alloys are compared with the relevant experimental data in Figure 5. Figure 6 shows the comparison between the calculated manganese activities at 800 °C, 1000 °C, and 1200 °C and experimental data at several temperatures by various authors.<sup>[28–32]</sup> The reference state of pure Mn is  $\beta$ -Mn. There is a severe discrepancy among individual investigators. The calculated activity lines show good agreement only with Zaitsev *et al.*'s data,<sup>[32]</sup> which is the only data set included in the optimization procedure, as mentioned already. Another comparison between the calculated manganese activities and experimental data by Zaitsev *et al.* is shown in Figure 7. Figure 7 shows that the present calculation reproduces the abrupt change in manganese activity along temperature at a constant composition reasonably well.

The calculated ferrite (bcc)/austenite (fcc) equilibria

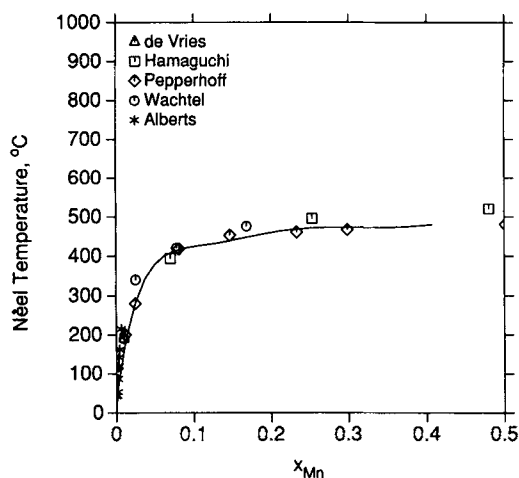


Fig. 5—The calculated Néel temperature of the bcc Cr-Mn alloys in comparison with experimental data (8,33–36).

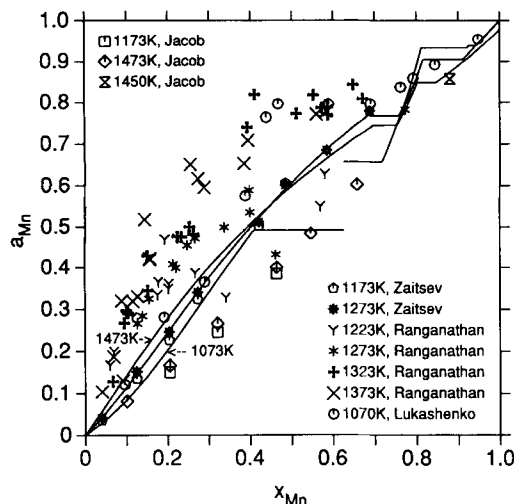


Fig. 6—The calculated activity of Mn in the solid Cr-Mn alloys at 1073, 1273, and 1473 K in comparison with experimental data (28–32). The reference state of pure Mn is  $\beta$ -Mn.

at 950 °C, 900 °C, 850 °C, 800 °C, and 750 °C in the Fe-Cr-Mn ternary system are compared in Figures 8 through 12 with experimental data by Kirchner and Uhrenius.<sup>[7]</sup> It was impossible to obtain good agreements with experimental data both in phase boundaries and direction of tie-lines. In the present assessment, the phase boundary information was given more weight. Thus, the agreement in the direction of tie-lines is rather poor while that in the phase boundaries is satisfactory. Figure 13 shows the calculated isothermal section of the Fe-Cr-Mn system at 650 °C. Experimental data on the fcc/ $\sigma$  equilibria by various authors are also presented for comparison. The experimental data by Okazaki *et al.*<sup>[31]</sup> and Abe *et al.*<sup>[12]</sup> show good agreement with the present calculation. However, there is a rather big discrepancy between calculation and Murata *et al.*'s data.<sup>[43]</sup> First, the phase boundary between the fcc and  $\alpha$ -Mn phase in the Fe-Mn binary side is different by several wt pct Mn from the present phase diagram of the Fe-Mn system.<sup>[12]</sup> Second,

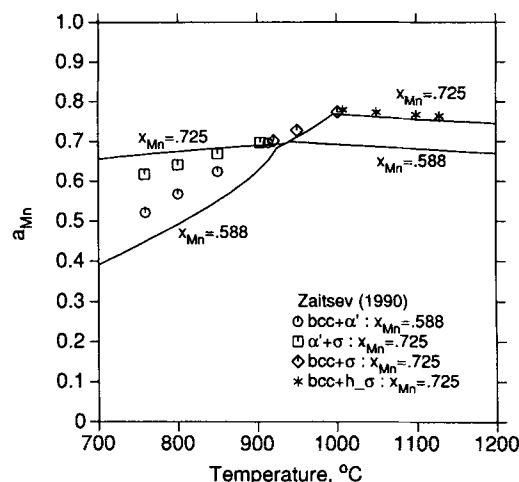


Fig. 7—The calculated activity of Mn in the solid Cr-Mn alloys at 58.8 and 72.5 wt pct Mn in comparison with experimental data (32). The reference state of pure Mn is  $\beta$ -Mn.

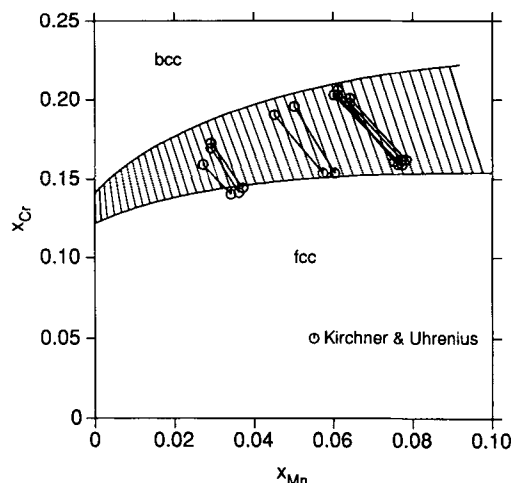


Fig. 8—The calculated ferrite (bcc)/austenite (fcc) equilibria at 950 °C in the Fe-Cr-Mn system in comparison with experimental data (7).

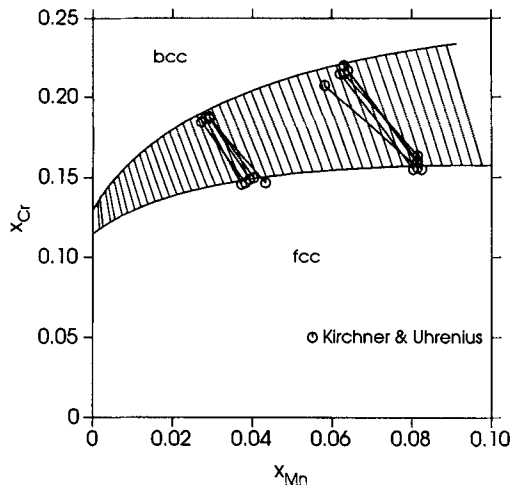


Fig. 9—The calculated ferrite (bcc)/austenite (fcc) equilibria at 900 °C in the Fe-Cr-Mn system in comparison with experimental data (7).

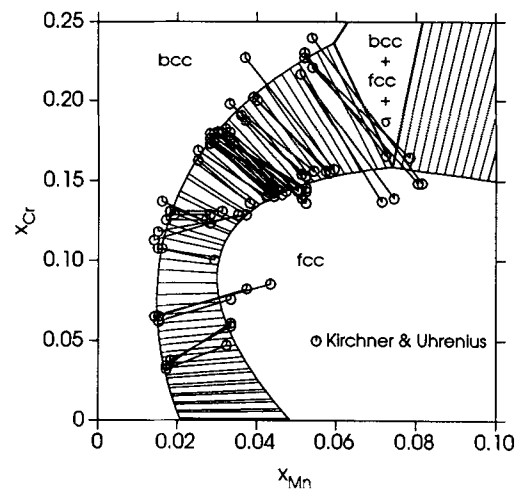


Fig. 12—The calculated ferrite (bcc)/austenite (fcc) equilibria at 750 °C in the Fe-Cr-Mn system in comparison with experimental data (7).

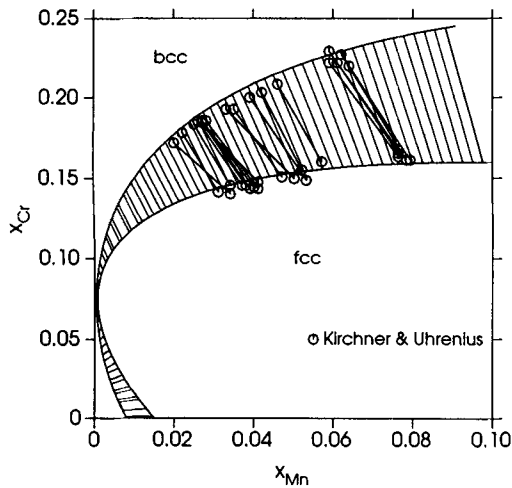


Fig. 10—The calculated ferrite (bcc)/austenite (fcc) equilibria at 850 °C in the Fe-Cr-Mn system in comparison with experimental data (7).

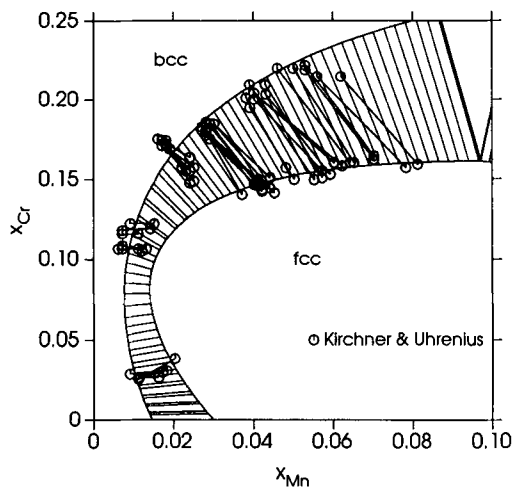


Fig. 11—The calculated ferrite (bcc)/austenite (fcc) equilibria at 800 °C in the Fe-Cr-Mn system in comparison with experimental data (7).

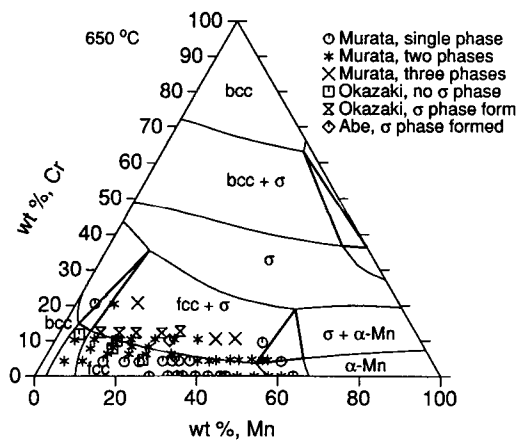


Fig. 13—The calculated isothermal section of the Fe-Cr-Mn system at 650 °C in comparison with experimental data (43,2,3).

according to Murata *et al.*'s data, the fcc/fcc +  $\sigma$  phase boundary should lie on a lower Cr content region at Fe-rich corner than in the present calculation. Disagreement in the fcc/fcc +  $\alpha$ -Mn/ $\alpha$ -Mn ternary phase boundaries that comes from disagreement in the Fe-Mn binary is inevitable in the present work. The Fe-Mn binary system would have to be reassessed considering Murata *et al.*'s data to remove these disagreements. However, it seems appropriate to wait before making such changes until more detailed and extensive experimental data are available on the Fe-Mn binary system.

A possible explanation for the disagreement in the fcc/fcc +  $\sigma$  phase boundary at the Fe-rich corner can be made as follows. A metastable  $\epsilon$  martensite (hcp) phase has been reported experimentally.<sup>[4,42,43,61]</sup> In Murata *et al.*'s article,<sup>[43]</sup> the microstructures of solution-treated alloys showed well-developed fcc +  $\epsilon$  two-phase type especially in the Fe-rich alloys. The authors also noted that in some specimens with relatively low Mn content, the  $\epsilon$  phase retained even after long annealing at 650 °C. Since the stability of the  $\epsilon$  phase is lower than the fcc phase, the metastable phase boundary  $\epsilon/\epsilon + \sigma$  should

be located in a lower Cr region than the stable phase boundary fcc/fcc +  $\sigma$ . Thus, if the  $\sigma$  phase had precipitated in equilibrium with the metastable  $\epsilon$  phase not in equilibrium with the stable fcc phase, then it would be possible to detect metastable  $\sigma$  phase in the fcc single-phase region. Due to slow kinetics, a long time would be needed for the metastable  $\sigma$  precipitates to resolve into the fcc phase even after the  $\epsilon$  phase transformed to the stable fcc phase. The severe scattering in the Cr contents of the  $\sigma$  precipitates (13 to 31 wt pct Cr) in Murata *et al.*'s work indicates that the precipitated  $\sigma$  phase is in incomplete equilibrium state. A conclusion can thus be made that the stability of the  $\sigma$  phase might be overestimated due to the occurrence of the metastable  $\epsilon$ (hcp) martensite. The experimental data by the same authors<sup>[4]</sup> on the fcc/ $\sigma$  equilibria at 800 °C also show disagreements in the location of the fcc/fcc +  $\sigma$  phase boundary from the present calculation, as shown in Figure 14. However, the 850 °C isothermal section in Figure 15 shows a slight disagreement but in the opposite direction

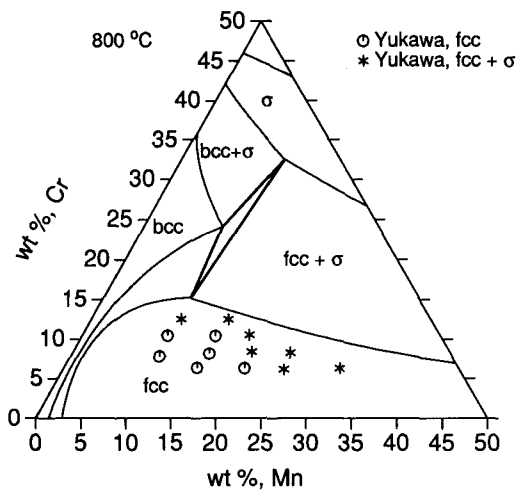


Fig. 14—The calculated isothermal section of the Fe-Cr-Mn system at 800 °C in comparison with experimental data (4).

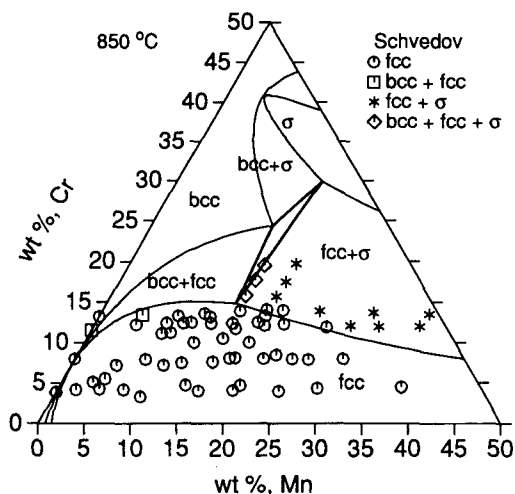


Fig. 15—The calculated isothermal section of the Fe-Cr-Mn system at 850 °C in comparison with experimental data (41).

between the present calculation and another experimental data set.<sup>[41]</sup> Figure 16 shows the calculated isothermal section of the Fe-Cr-Mn system at 1000 °C.

The vertical sections of the Fe-Cr-Mn system at 6, 16, and 28 wt pct Mn are also calculated and compared with experimental data by Grigor'ev and Gruzdeva<sup>[39]</sup> in Figures 17 through 19. The agreement between calculation and experimental data is generally poor and even bad especially in the 28 pct Mn section (Figure 19). However, it should be noted that the annealing time at 600 °C was only 170 hours in the previous experimental work,<sup>[39]</sup> and the present calculation of the fcc/bcc phase boundary shows rather good agreement with recent data by Okazaki *et al.*<sup>[42]</sup> in the temperature range of 1000 °C to 1200 °C.

There is good agreement between the present calculation and the experimental data on the liquidus temperatures in the Fe-rich region of the Fe-Cr-Mn system by Kundrat,<sup>[44]</sup> as shown in Figure 20. In Figure 20, the numbers represent the difference between the melting point of pure iron (1811 K) and the liquidus temperature at

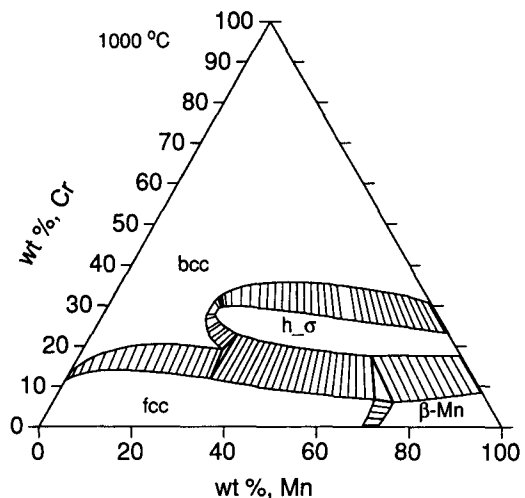


Fig. 16—The calculated isothermal section of the Fe-Cr-Mn system at 1000 °C.

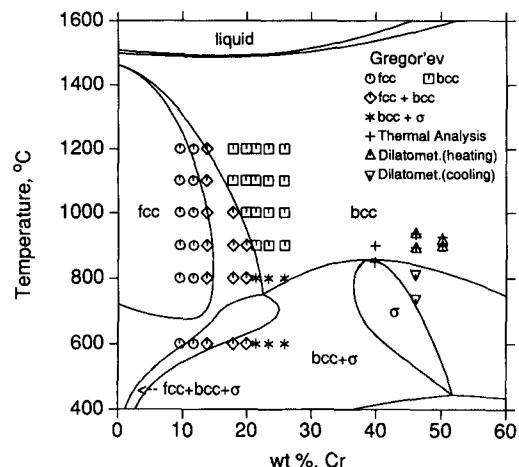


Fig. 17—The calculated vertical section of the Fe-Cr-Mn system at 6 wt pct Mn in comparison with experimental data (39).

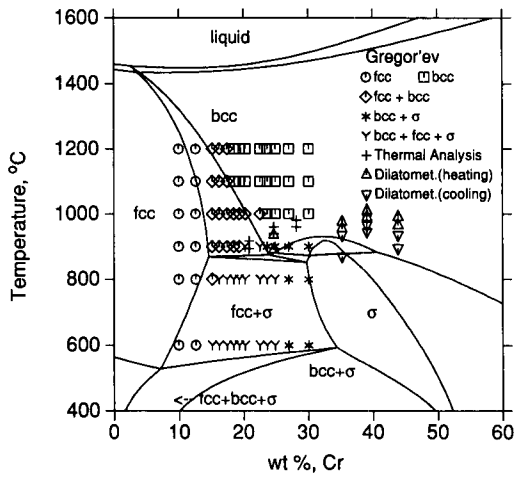


Fig. 18—The calculated vertical section of the Fe-Cr-Mn system at 16 wt pct Mn in comparison with experimental data (39).

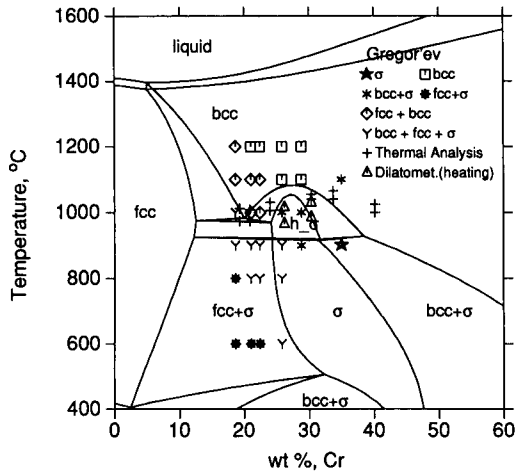


Fig. 19—The calculated vertical section of the Fe-Cr-Mn system at 28 wt pct Mn in comparison with experimental data (39).

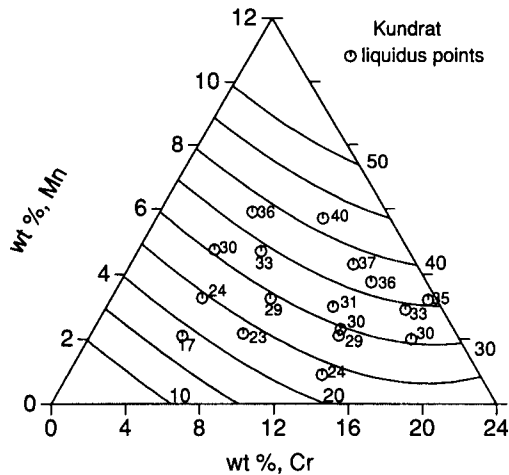


Fig. 20—The calculated liquidus surface in the Fe-rich region of the Fe-Cr-Mn system in comparison with experimental data (44). The numbers represent the difference between the melting point of pure iron (1811 K) and the liquidus temperature at each composition or line.

each composition or line. Thus, the line denoted with "30" is the calculated liquidus line at 1781 K, and the data point denoted with "40" means that the experimental liquidus point at that composition is 1771 K, for example. Figure 21 shows the calculated isothermal sections at 1786, 1781, and 1776 K in comparison with some experimental tie-lines between liquid and bcc by the same author.<sup>[44]</sup> The agreement is rather good in the Fe-Mn binary side but poor in the Fe-Cr binary side. The temperature differences between liquidus and solidus lines are much smaller in the Fe-20 pct Cr region than in the Fe-5 pct Mn region; thus, it would be more difficult to measure tie-lines exactly in the Fe-20 pct Cr region. However, there is relatively good agreement in the liquidus temperatures even in the Fe-Cr binary side. Finally, Figure 22 shows the calculated liquidus projections of the Fe-Cr-Mn system in the whole composition range. In Figure 22, the tick mark numbers  $Z$  give the temperatures according to the relation:  $T (^{\circ}\text{C}) = 1200 + 30Z$ .

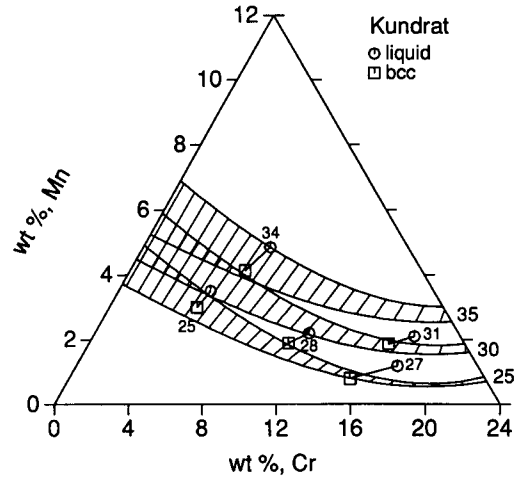


Fig. 21—The calculated isothermal sections at 1786, 1781, and 1776 K in the Fe-rich region of the Fe-Cr-Mn system in comparison with experimental data (44). The numbers represent the difference between the melting point of pure iron (1811 K) and the liquidus temperature at each composition or line.

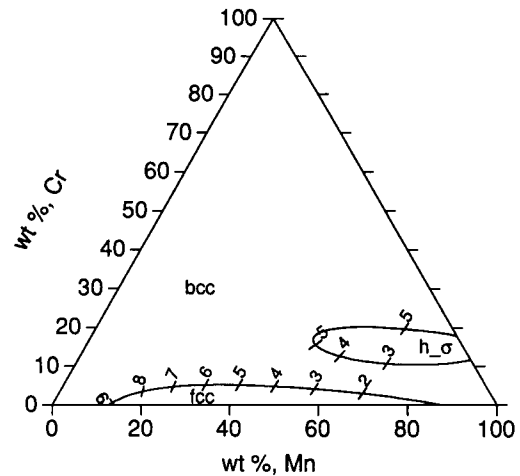


Fig. 22—The calculated liquidus projections of the Fe-Cr-Mn system. The number  $Z$  give the temperatures according to  $T (^{\circ}\text{C}) = 1200 + 30Z$ .

## VI. SUMMARY AND CONCLUSIONS

A thermodynamic evaluation of the Cr-Mn and Fe-Cr-Mn systems has been made by using thermodynamic models for the Gibbs energy of individual phases. The Cr-Mn binary system could be assessed successfully by assuming two different sigma phases and using a different thermodynamic description for each sigma phase. The model parameters for the two ternary sigma phases could be obtained rather simply by assuming the same effect of Fe on the thermodynamic properties of both phases. Several isothermal and vertical sections in the Fe-Cr-Mn system were calculated using the optimized thermodynamic parameters and are presented for comparison with relevant experimental data.

## ACKNOWLEDGMENT

The author wishes to thank Professor Mats Hillert and Dr. Bo Sundman at the Royal Institute of Technology, Sweden, for the valuable discussion during this work. This work has been financially supported partly by the Korean Ministry of Science and Technology and partly by the Swedish Board for Technical Development.

## REFERENCES

- H.R. Brager, F.A. Garner, D.S. Gelles, and M.L. Hamilton: *J. Nucl. Mater.*, 1985, vols. 133-34, pp. 907-11.
- F. Abe, H. Araki, and T. Noda: *Mater. Sci. Technol.*, 1988, vol. 4, pp. 885-93.
- Y. Okazaki, K. Miyahara, Y. Hosoi, M. Tanino, and H. Komatsu: *J. Jpn. Inst. Met.*, 1989, vol. 53, pp. 512-21.
- N. Yukawa, M. Morinaga, K. Nishiyama, Y. Matsumoto, Y. Murata, and H. Ezaki: ASTM STP 1047, R.E. Klueh, D.S. Gelles, M. Okada, and N.H. Packen, eds., ASTM, Philadelphia, PA, 1990, pp. 30-46.
- C.O. Burgess and W.D. Forgeng: *Trans. AIME.*, 1938, vol. 131, pp. 277-99.
- P. Schafmeister and R. Ergang: *Arch. Eisenhüttenwes.*, 1939, vol. 12, pp. 507-10.
- G. Kirchner and B. Uhrenius: *Acta Metall.*, 1974, vol. 22, pp. 523-32.
- E. Wachtel and C. Bartelt: *Z. Metallkd.*, 1964, vol. 55, pp. 29-36.
- M. Venkatraman and J.P. Neumann: *Bull. Alloy Phase Diagrams*, 1986, vol. 7, pp. 457-62.
- L. Kaufman: *CALPHAD*, 1978, vol. 2, pp. 117-46.
- J.-O. Andersson: *CALPHAD*, 1987, vol. 11, pp. 83-92.
- W. Huang: *CALPHAD*, 1989, vol. 13, pp. 243-52.
- M. Hillert and L.I. Staffansson: *Acta Chem. Scand.*, 1970, vol. 24, pp. 3618-26.
- B. Sundman and J. Ågren: *J. Phys. Chem. Solids*, 1981, vol. 42, pp. 297-301.
- G. Inden: *Bull. Alloy Phase Diagrams*, 1981, vol. 2, pp. 412-22.
- M. Hillert and M. Jarl: *CALPHAD*, 1978, vol. 2, pp. 227-38.
- J.-O. Andersson, A. Fernández Guillermet, M. Hillert, B. Jansson, and B. Sundman: *Acta Metall.*, 1986, vol. 34, pp. 437-45.
- I.I. Kornilov and A.I. Tatyanchikova: *Dokl. Akad. Nauk SSSR*, 1945, vol. 50, pp. 223-25.
- S.J. Carlile, J.W. Christian, and W. Hume-Rothery: *J. Inst. Met.*, 1949, vol. 76, pp. 169-94.
- A. Dinsdale: "SGTE Data for Pure Element," NPL Report DMA(A) 195, Rev. Aug. 1990.
- W.B. Pearson, J.W. Christian, and W. Hume-Rothery: *Nature*, 1951, vol. 167, p. 110.
- H.T. Greenaway, S.T.M. Johnstone, and M.K. McQuillan: *J. Inst. Met.*, 1951, vol. 80, pp. 109-14.
- U. Zwicker: *Z. Metallkd.*, 1951, vol. 42, pp. 277-78.
- W.B. Pearson and W. Hume-Rothery: *J. Inst. Met.*, 1952, vol. 81, pp. 311-14.
- A. Hellawell and W. Hume-Rothery: *Phil. Trans. R. Soc. London*, 1957, vol. A-249, pp. 417-59.
- E. Lugscheider and P. Ettmayer: *Monatsh. Chem.*, 1971, vol. 102, pp. 1234-44.
- V.N. Eremenko, G.M. Lukashenko, and V.R. Sidorko: *Russ. J. Phys. Chem.*, 1968, vol. 42, pp. 343-46.
- K.T. Jacob: *Z. Metallkd.*, 1985, vol. 76, pp. 415-19.
- S. Ranganathan and J.P. Hajra: *Metall. Trans. B*, 1988, vol. 19B, pp. 649-54.
- S. Ranganathan and J.P. Hajra: *Scripta Metall.*, 1988, vol. 22, pp. 13-16.
- G.M. Lukashenko and V.R. Sidorko: *Izv. Akad. Nauk SSSR, Metall.*, 1989, pp. 28-30.
- A.I. Zaitsev, M.A. Zemchenko, and B.M. Mogutnov: *J. Chem. Thermodynamics*, 1990, vol. 22, pp. 41-53.
- G. de Vries: *J. Phys. Radium*, 1959, vol. 20, pp. 438-39.
- Y. Hamaguchi and N. Kunitomi: *J. Phys. Soc. Jpn.*, 1964, vol. 19, pp. 1849-56.
- W. Pepperhoff and H.H. Ettwig: *Z. Angew. Phys.*, 1968, vol. 24, pp. 88-90.
- H.L. Alberts and J.A.J. Lourens: *J. Phys. F: Met. Phys.*, 1987, vol. 17, pp. 727-30.
- W. Köster: *Arch. Eisenhüttenwes.*, 1933-1934, vol. 7, pp. 687-88.
- M. Schmidt and H. Legat: *Arch. Eisenhüttenwes.*, 1936-1937, vol. 10, pp. 297-306.
- A. Grigor'ev and N.M. Gruzdeva: *Akad. Nauk SSSR, Izv. Sekts. Fiz.-Khim. Analiz.*, 1949, vol. 18, pp. 92-116.
- F.N. Tavazde, V.A. Pirtskhalaishvili, and M.A. Nabichvrishvili: *Soobsh. Akad. Nauk Gruz. SSR*, 1968, vol. 49, pp. 641-46.
- L.I. Shvedov and Z.D. Pavlenko: *Izvest. Akad. Nauk Beloruss. SSR*, 1975, pp. 22-27.
- Y. Okazaki, K. Miyahara, N. Wade, and Y. Hosoi: *J. Jpn. Inst. Met.*, 1989, vol. 53, pp. 502-11.
- Y. Murata, K. Koyama, Y. Matsumoto, M. Morinaga, and N. Yukawa: *Iron Steel Inst. Jpn. Int.*, 1990, vol. 30, pp. 927-36.
- D.M. Kundrat: *Metall. Trans. A*, 1986, vol. 17A, pp. 1825-35.
- K. Mukai, A. Uchida, T. Tagami, and Y. Wasai: *Proc. 3rd Int. Iron and Steel Congress*, ASM, Metals Park, OH, 1978, pp. 266-76.
- B. Jansson: Ph.D. Thesis, Royal Institute of Technology, Stockholm, Sweden, 1984.
- A. Fernández Guillermet and P. Gustafson: *High Temp.-High Press.*, 1985, vol. 16, pp. 591-610.
- J.-O. Andersson: *Int. J. Thermophys.*, 1985, vol. 6, pp. 411-19.
- J.-O. Andersson, A. Fernández Guillermet, and P. Gustafson: *CALPHAD*, 1987, vol. 11, pp. 361-64.
- A. Fernández Guillermet and W. Huang: *Int. J. Thermophys.*, 1990, vol. 11, pp. 949-69.
- N. Saunders, A.P. Miodownik, and A.T. Dinsdale: *CALPHAD*, 1988, vol. 12, pp. 351-74.
- S.K. Lee and D.N. Lee: *CALPHAD*, 1986, vol. 10, pp. 61-75.
- K. Fritscher and H. Hammelrath: *Naturwiss.*, 1984, vol. 71, p. 583.
- B.-J. Lee: *CALPHAD*, 1992, vol. 16, pp. 121-49.
- M. Hillert and C. Qiu: *Metall. Trans. A*, 1990, vol. 21A, pp. 1673-80.
- B.-J. Lee: *CALPHAD*, 1993, vol. 17, pp. 251-68.
- L.I. Shvedov and Z.D. Pavlenko: *Izvest. Akad. Nauk Beloruss. SSR*, 1975, pp. 14-17.
- B. Potucek: *Hutnicke Listy*, 1958, vol. 13, pp. 1070-76.
- V.G. Rivlin and G.V. Raynor: *Int. Met. Rev.*, 1983, vol. 28, pp. 23-64.
- F.D. Lemkey, E.R. Thompson, J.C. Schuster, and H. Nowotny: *Mater. Res. Soc. Symp. Proc.*, 1982, pp. 31-50.
- I. Ya Georgieva, N.A. Sorokina, and V.I. Gal'tsova: *Fiz. Met. Metalloved.*, 1980, vol. 49, pp. 206-09.
- K. Frisk: *Metall. Trans. A*, 1990, vol. 21A, pp. 2477-88.
- B. Sundman, B. Jansson, and J.-O. Andersson: *CALPHAD*, 1985, vol. 9, pp. 153-90.